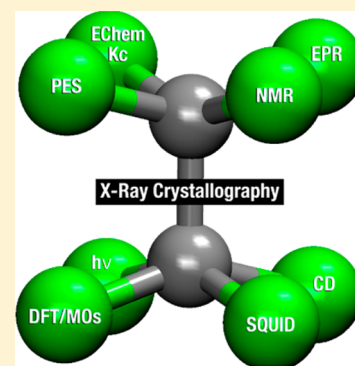


Fitting the Pieces of the Puzzle: The  $\delta$  BondLarry R. Falvello,<sup>\*,†</sup> Bruce M. Foxman,<sup>\*,‡</sup> and Carlos A. Murillo<sup>\*,§,⊥</sup><sup>†</sup>Departamento de Química Inorgánica, ICMA, Universidad de Zaragoza, CSIC, Pedro Cerbuna 12, E-50009 Zaragoza, Spain<sup>‡</sup>Department of Chemistry, MS 015, Brandeis University, Waltham, Massachusetts 02453, United States<sup>§</sup>Department of Chemistry, Texas A&M University, P.O. Box 30012, College Station, Texas 77842-3012, United States<sup>⊥</sup>Department of Chemistry, University of Texas at El Paso, El Paso, Texas 79968, United States

**ABSTRACT:** The development of our understanding of the  $\delta$  bond and its role in quadruple metal–metal bonding is described in terms of the conceptual advances and experimental and theoretical results achieved through a 50-year period beginning with the seminal report by Cotton and co-workers in 1964. The work behind the original discovery is described, along with the qualitative orbital description of the components of the quadruple bond. The effect of torsion about the metal–metal axis on the metal–metal bond length is described, together with the conclusion that this accords with a progressive loss of the  $\delta$  component of the metal–metal bond. The important role of photoelectron spectroscopy in characterizing the loss of electrons from the metal–metal bonding orbitals is reviewed, as are the electron paramagnetic resonance results that establish that unpaired electrons, when present, populate metal-based orbitals. Other important results are described: destabilization of the metal–metal bond to produce strong reducing agents, exceptions to the expected orbital ordering, and the use of chiroptical properties to reveal additional information about the electronic structure of the metal–metal bond.



## ■ INTRODUCTION

When F. Albert Cotton (Al to all who knew him) began his independent career in September of 1955 as an Instructor at Massachusetts Institute of Technology—a short trip across town from Harvard, where he had just finished his Ph.D. under the direction of Geoff Wilkinson—preparing a compound with a quadruple bond was not in his plans. As many readers would know, there were already some quadruple-bonded compounds in the literature, which at the time remained unrecognized as such. An example, chromium(II) acetate, was reported by Peligot<sup>1</sup> as  $\text{CrC}_4\text{H}_4\text{O}_5$  in 1844, with this odd formula owing to uncertainties prevalent at the time regarding the atomic and molecular weights of hydrogen.

In his early career, Al was fascinated by symmetry and NMR spectroscopy, as demonstrated in one of his early papers, in which he examined the structure of  $\text{SF}_4$  by IR and  $^{19}\text{F}$  NMR.<sup>2</sup> This compound has  $C_{2v}$  as opposed to  $T_d$  symmetry, and its structure is derived from a trigonal bipyramid, with the electron pair occupying one of the equatorial positions. He then became interested in transition-metal carbonyls because the CO stretching frequencies<sup>3</sup> as well as  $^{13}\text{C}$  NMR provided excellent handles for structural studies.<sup>4</sup> It should be noted that at the time  $^{13}\text{C}$  NMR was not at all a routine technique. Al then went on to study a series of what today would be considered common species, namely, acetylacetonates with transition metals,  $\text{M}(\text{acac})_2$ , many of which were not simply mononuclear but rather oligomeric compounds.<sup>5</sup>

■ EARLY STORY OF THE  $\delta$  BOND IN QUADRUPLE-BONDED SPECIES

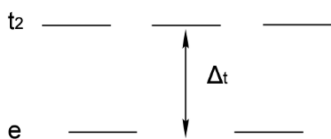
In 1962–1963, there was an event that Al considered spectacular and career-changing. This occurred when X-ray crystallography was in its infancy, rather than the routine tool it is today. Al decided to take a look at a structure that had been known in the literature as “ $\text{CsReCl}_4$ ”, presumably containing a tetrahedral species in a low-spin ground state. As any inorganic textbook would indicate today, low-spin tetrahedral species have been elusive and still remain unknown.<sup>6</sup> As Al told the story, the molecule had a lot in its favor for becoming the first  $T_d$  structure of a heavy-transition-metal complex. It had a third-row transition-metal atom, which would increase the orbital separation and thus have a maximal ligand-field splitting, and it also had four electrons, which would give a closed  $e^4t^0$  configuration that would be consistent with the observed diamagnetism (see Scheme 1). The solution of the structure proved to be quite a challenge in those precomputer days when intensity data were collected on photographic film, as opposed to today’s electronic area detectors. Nevertheless, it was quickly found that no tetrahedral  $\text{ReCl}_4^-$  anions, in fact, were present! Instead, a structure with three rhenium atoms in close proximity (ca. 2.50 Å) was observed.<sup>7</sup> In the plane of the triangle of metal atoms, there were three chlorine atoms, each bridging two rhenium atoms. In addition, each metal atom was bonded to three terminal chlorine atoms, as shown in Figure 1. Al and his co-workers were astonished to find a metal-to-metal

Received: January 17, 2014

Published: September 15, 2014



**Scheme 1. Expected Crystal-Field Splitting for a Tetrahedral ( $T_d$ )  $ML_4$  Species<sup>a</sup>**



<sup>a</sup>The e state corresponds to the  $d_{x^2-y^2}$  and  $d_{z^2}$  orbitals, while the  $t_2$  state corresponds to the  $d_{xy}$ ,  $d_{xz}$ , and  $d_{yz}$  triplet of orbitals from the transition-metal atom. The difference in energy is expressed as  $\Delta_t$ .

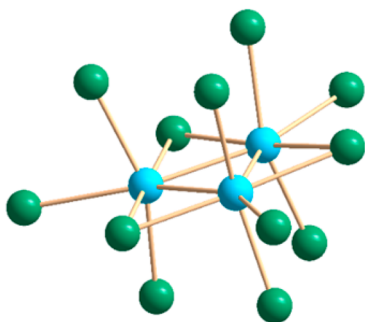


**Figure 1.** Structure of the triangular anion in  $Cs_3Re_3Cl_{12}$ , where each of the  $Re=Re$  bonds has a bond order of 2.

distance in this  $Cs_3Re_3Cl_{12}$  compound that was 0.26 Å shorter than that in rhenium metal (2.76 Å). This led to the conclusion that there were  $Re=Re$  double bonds, which was an unprecedented result.

Following this discovery, Al and his group went on to investigate what he referred to as a “conundrum of strange properties” in rhenium(III) chloride, a compound that was insoluble when freshly prepared but much more soluble after exposure to air. The compound could be treated with a large number of neutral ligands, giving new species of unknown composition. This is when Al’s student Joel Mague came into the picture to clear up the confusion. It was found that the so-called  $ReCl_3$  had a structure similar to that of  $Cs_3Re_3Cl_{12}$  but, of course, without the cesium atoms.<sup>8</sup> To avoid being coordinatively unsaturated, the structure formed infinite sheets with bridging chlorine atoms, but in the presence of neutral molecules such as phosphines, soluble species such as  $Re_3Cl_9(PEt_2Ph)_3$  gave molecular species (Figure 2), which explained the change in solubility.<sup>9</sup>

By then, the “bug” that carried the metal-to-metal bond fever had forever infected Al. His graduate student Steve Lippard went on show that the structure of  $ReBr_3$  was similar to that of the chlorine analogue.<sup>10</sup> At this point, one of us came into the picture to study the iodo species, but in Al’s words “the problem with  $ReI_3$  proved recalcitrant ... since the stuff just seemed bent on dying a non-crystalline death.” After a long battle, the structure was finally solved, also revealing trinuclear clusters but linked differently so that one rhenium atom in each cluster remained coordinatively unsaturated, as seen in Figure 3.<sup>11</sup> The unsaturation leads to  $Re-Re$  distances that are not equal. The two longest distances (2.507 Å) are in the nondeficient (seven-coordinate) rhenium atoms, while the short bond (2.440 Å) is associated with the six-coordinate rhenium atom.

Intertwined with Al’s interest in horses and hounds, his love for his new wife Dee, and the planning of a visit to Buenos Aires, there appeared some confusing results in the Russian

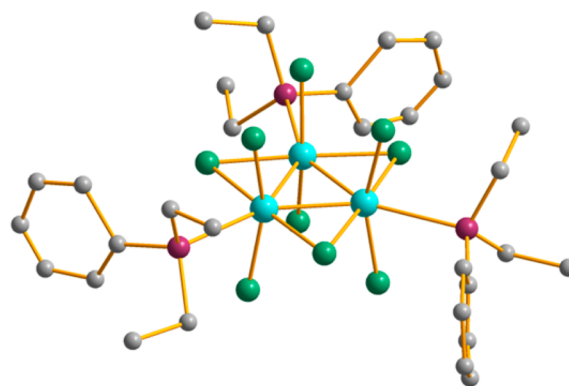


**Figure 2.** Structure of the neutral compound  $Re_3Cl_9(PEt_2Ph)_3$ , showing the triangular arrangement of the rhenium atoms, drawn using a light-blue color.

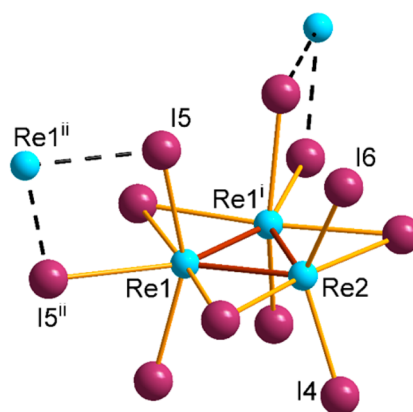


**Figure 3.** Structure of  $Re_3I_9$ , showing that one of the rhenium atoms,  $Re_2$ , is coordinatively unsaturated. A chain of linked trinuclear units is propagated at the  $I5/I5''$  bridges. Symmetry codes:  $i, x, 0.5 - y, z$ ;  $ii, -x, 1 - y, -z$ .

literature describing compounds with a variety of interesting formulations, e.g.,  $H_2ReCl$ ,  $KHReCl_4$ ,  $ReCl_2 \cdot 2H_2O$ ,  $H_2ReCl_4 \cdot 2H_2O$ , and  $KHReCl_4 \cdot 2H_2O$ . Al’s student Charles Harris began to examine “ $KReCl_4 \cdot H_2O$ ” crystallographically, but then a paper appeared in *Zh. Strukt. Khim.* reporting a compound with the formula “ $(pyH)HReCl_4$ ”. Steve Lippard, who knew Russian, translated the report, which described a compound with two rhenium atoms lying within a square prism; each rhenium atom was bonded to four chlorine atoms, and the distance between metal atoms was only 2.22 Å. However, there was a considerable mixup as to the nature of the hydrogen atoms owing to problems with severe crystallographic disorder. In the *Zh. Strukt. Khim.* report, the anion was described as being  $[Re_2Cl_8]^{4-}$ . This prompted an immediate reevaluation by a team in Al’s group. The team was composed of Neil Curtis, Charles Harris, Brian Johnson, Steve Lippard, Joel Mague, Bill Robinson, and John Wood.

The literature synthesis was repeated, but new synthetic methods were also developed.<sup>12</sup> The structure showed that the charge was not 4− but instead 2−, i.e.,  $[Re_2Cl_8]^{2-}$ . The charge is important because the dianion would provide eight metal-based d electrons instead of 10 in the tetraanion. This work brought about the seminal paper published in the September 18, 1964, issue of *Science* (50 years ago), explaining the structure shown in Figure 4.<sup>13</sup> With characteristic clarity, Al led

the readers of that initial report to the conclusion that a metal–metal quadruple bond was present:

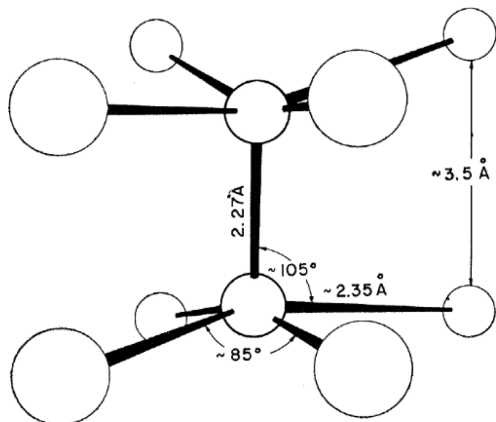


**Figure 4.** Structure of the  $[\text{Re}_2\text{Cl}_8]^{2-}$  anion as published in *Science* (ref 13). This is a hand drawing done by Charles Harris.

“The fact that  $[\text{Re}_2\text{Cl}_8]^{2-}$  has an eclipsed, rather than staggered, structure (that is, not the structure to be expected on considering only the effects of repulsions between chlorine atoms) is satisfactorily explained when the Re–Re multiple bonding is examined in detail. To a first approximation, each rhenium atom uses a set of  $s$ ,  $p_x$ ,  $p_y$ ,  $d_{x^2-y^2}$  hybrid orbitals to form its four Re–Cl bonds. The remaining valence shell orbitals of each rhenium may then be used for metal-to-metal bonding as follows: (i) On each rhenium,  $d_{z^2-p_z}$  hybrids overlap to form a very strong  $\sigma$  bond. (ii) The  $d_{xz}$ ,  $d_{yz}$  pair on each rhenium can be used to form two fairly strong  $\pi$ -bonds. Neither the  $\sigma$  nor the  $\pi$  bonds impose any restriction on rotation about the Re–Re axis. These three bonding orbitals will be filled by six of the eight Re  $d$  electrons. (iii) There remains now, on each rhenium atom, a  $d_{xy}$  orbital containing one electron. In the eclipsed configuration these overlap to a fair extent (about one third as much as one of the  $\pi$  overlaps) to give a  $\delta$  bond, with the two electrons becoming paired. This bonding scheme is in accord with the measured diamagnetism of the  $[\text{Re}_2\text{Cl}_8]^{2-}$  ion. If, however, the molecule were to have a staggered configuration, the  $\delta$  bonding would be entirely lost ( $d_{xy}-d_{xy}$  overlap would be zero)... Since the Cl–Cl repulsion energy tending to favor the staggered configuration can be estimated to be only a few kilocalories per mole, the  $\delta$ -bond energy is decisive and stabilizes the eclipsed configuration. This would appear to be the first quadruple bond to be discovered.”

Pictorially, a basic molecular orbital (MO) diagram can be drawn to represent the above description, and this is shown in Figure 5. Owing to the insolubility and lack of crystallinity of the triphenylphosphine substitution product,<sup>14</sup> the question of whether  $\text{Re}_2\text{Cl}_6\text{P}_2$  species retained the quadruple bond upon substitution remained unanswered until 1968, when the eclipsed, quadruple-bonded structure of the triethylphosphine derivative was published.<sup>15</sup> In the year following the initial discovery, a flurry of activity was seen immediately, and the new results showed that rhenium was not unique because other metals could also form such compounds. Knowing the structure of the  $[\text{Re}_2\text{Cl}_8]^{2-}$  anion, Al recognized that a technetium halide compound prepared a year earlier could have a similar structure.<sup>16</sup> He went on to work on this radioactive material using what was then for chemists the novel and complex

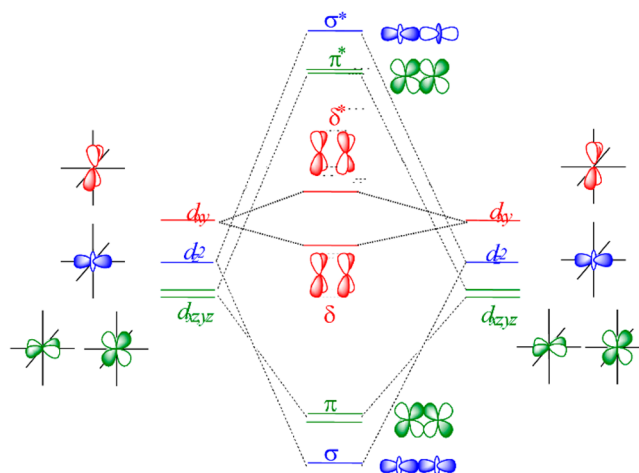


**Figure 5.** Schematic MO diagram for a  $D_{4h}$  species with two metal atoms such as that in the  $[\text{Re}_2\text{Cl}_8]^{2-}$  anion.

technique of single-crystal structure analysis and found that indeed  $(\text{NH}_4)_3\text{Tc}_2\text{Cl}_8$  had an anion structurally analogous to  $[\text{Re}_2\text{Cl}_8]^{2-}$ .<sup>17</sup> Importantly, the charge of the anion was 3– instead of 2–. Because rhenium and technetium have the same number of valence electrons, there is an additional electron in the anion, and thus the compound would be expected to be paramagnetic if the diagram in Figure 5 were to be correct. Indeed, the technetium compound was found to have an unpaired electron. In the same issue of the journal describing the structure of the ditechneum complex, and back to back with that paper, was the report of the structure of dimolybdenum tetraacetate, in which two molybdenum atoms are bonded to each other at a distance of 2.11 Å. This neutral species had four acetate bridging ligands.<sup>18</sup> This is what today we refer to as a *paddlewheel structure* by analogy with the regularly spaced paddles characteristically found at the rear of steamboats. At the time, Al indicated that it “appears that the formation of extremely short, presumably quadruple, bonds between  $d^4$  ions of the second- and third-row transition elements may be quite general.”<sup>17</sup> From that point on, vast amounts of time and effort were devoted to determining whether this was correct and whether the MO diagram with an ordering of  $\sigma < \pi \ll \delta < \delta^* \ll \pi^* < \sigma^*$  was adequate and indeed explained the properties of other dimetal units having true or idealized  $D_{4h}$  symmetry.

There are now hundreds of papers in this field describing studies including synthesis, as well as crystallographic, spectroscopic [IR, UV/vis, NMR, electron paramagnetic resonance (EPR), X-ray photoelectron spectroscopy (XPS), etc.], electrochemical, magnetic, and theoretical characterization, along with studies involving many other techniques.<sup>19</sup> As of this date, there are  $[\text{M}_2\text{X}_8]^{n-}$  species known for  $\text{M} = \text{Mo}$ ,  $\text{W}$ ,  $\text{Tc}$ ,  $\text{Re}$ , and  $\text{Os}$ . When tetragonal or trigonal paddlewheel compounds (having the same metal atoms) are considered with various ligands such as carboxylates, amidates, formamidates, guanidates, and others, there are paddlewheel compounds known with metal-to-metal bonds for  $\text{M} = \text{V}$ ,  $\text{Nb}$ ,  $\text{Cr}$ ,  $\text{Mo}$ ,  $\text{W}$ ,  $\text{Tc}$ ,  $\text{Re}$ ,  $\text{Fe}$ ,  $\text{Ru}$ ,  $\text{Os}$ ,  $\text{Co}$ ,  $\text{Rh}$ ,  $\text{Ir}$ ,  $\text{Ni}$ ,  $\text{Pd}$ , and  $\text{Pt}$ . In such compounds, bond orders vary from 0.5 to 4. For these compounds, the formal bond order (b.o.) is defined as the number of electrons in bonding orbitals (see Figure 5) minus those in antibonding orbitals, divided by 2.

$$\text{b.o.} = \frac{n(\text{bonding}) - n(\text{antibonding})}{2}$$

For the purpose of this Viewpoint Article, owing to the very extensive literature of metal–metal-bonded complexes from Al's group and others, we will describe only a few *key* experiments. The main idea of the selection is to help younger readers appreciate how a serendipitous discovery can be a game-changer if the investigator is capable of recognizing such an event and then of carrying out thoughtful and well-designed experiments to interrogate his or her hypothesis.

### ■ IS THE $\delta$ BOND TRULY AFFECTED BY ROTATION?

As mentioned, the paper we honor today, published 50 years ago, indicated that, should the  $[\text{Re}_2\text{Cl}_8]^{2-}$  dianion have a staggered configuration, the  $\delta$  bonding would be entirely lost because the  $d_{xy}-d_{xy}$  overlap would be zero.<sup>13</sup> To test this hypothesis, a series of experiments were designed involving dimolybdenum compounds with halides ( $X = \text{Cl}, \text{Br}$ ) and phosphines of the type  $\text{Mo}_2\text{X}_4(\text{P})_n$ ,  $n = 4$  if P is a monophosphine or  $n = 2$  if P is a diphosphine. The experiment was intended to test how the Mo–Mo distances changed as torsional strain was introduced by bridging diphosphines with concomitant diminution of the  $d_{xy}-d_{xy}$  overlap, i.e., the  $\delta$  bond. As the angle of rotation about the metal–metal bond— $\chi$ , the “internal twist”—progressed from zero for an eclipsed conformation to  $45^\circ$  for a staggered arrangement with no  $\delta$  bonding, what would be the effect on the metal–metal distance? In this progression, the formal bond order would decrease from 4 for zero torsion to 3 at  $\chi = 45^\circ$ . Such a decrease in the bond order should be reflected in a lengthening of the Mo–Mo distances.

As has been described in detail elsewhere,<sup>19</sup> the inverse relationship between the bond length and bond order is not as straightforward for bonds between metal atoms compared to those involving the elements carbon, nitrogen, and oxygen.<sup>20</sup> Especially when isolating the influence of the relatively weak  $\delta$  component of a quadruple bond, it is imperative to exclude variations in the other factors that have an observable effect on the M–M bond length, particularly the charge on the metals. In a carefully controlled analysis of the structures of 10 compounds with quadruple bonds—nine of the type  $\text{Mo}_2\text{X}_4(\text{P}^\wedge\text{P})_2$  ( $X = \text{Cl}$ , six compounds;  $X = \text{Br}$ , three compounds), plus one of the type  $\text{Mo}_2\text{Br}_4(\text{As}^\wedge\text{P})_2$ , in which ( $\text{P}^\wedge\text{P}$ ) and ( $\text{As}^\wedge\text{P}$ ) represent bridging diphosphine and arsinophosphine ligands, Al and co-workers traced the Mo–Mo bond length as a function of the twist angle about the metal–metal bond.<sup>21</sup> All of the compounds possess the generic structure shown in Figure 6; all are neutral, and all have four halide ligands and two neutral bridging ligands, with the length of the bridge varying along the series. The latter feature produces variable torsional stress, with the result that these otherwise analogous molecules have different twist angles about the metal–metal bond.

It had been established that the overlap between the  $d_{xy}$  orbitals of the two metal atoms—that is, the orbital overlap for the  $\delta$  component of the bond between them—varies as  $\cos 2\chi$ , in which  $\chi$  was taken, for the purpose of the analysis, as the average of the four smallest torsion angles about the M–M axis [ $X-M-M-X$  or  $P-M-M-(P, \text{As})$ ] (Figure 6a).<sup>22</sup> So, with the  $\delta$  component of the quadruple bond isolated as the only distance-influencing factor that varies across the series of 10 compounds, a plot of the Mo–Mo distance as a function of the

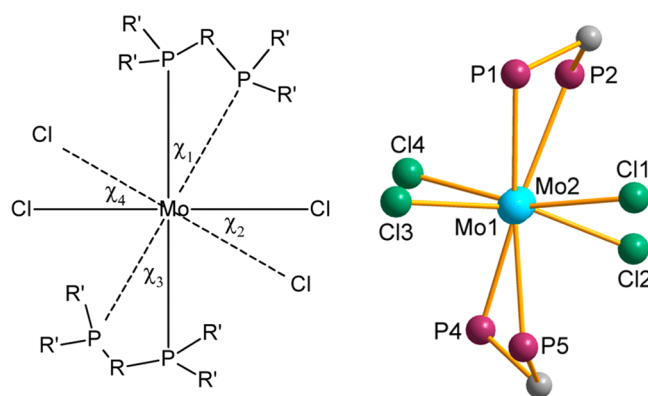


**Figure 6.** (a) Generic structure of compounds of the type  $\text{Mo}_2\text{X}_4(\text{P}^\wedge\text{P})_2$ . The bridgehead R is a one-, two-, or four-carbon-atom unit. The terminal groups R' of the phosphine can be aliphatic or aromatic. For the purposes of the analysis, the twist angle  $\chi$  is taken as the average of the four smallest torsion angles about the metal–metal bond. (b) Core of the molecule  $\text{Mo}_2\text{Cl}_4(\text{tdpm})_2$  [tdpm = tris(diphenylphosphino)methane].

twist angle should produce a linear plot. That was indeed the result, although the correlation coefficient of the fit, 0.916, indicated some scatter in the data. The extrapolated distance at the  $y$  intercept, 2.192 Å, provides an estimate of the Mo–Mo bond distance for a mean torsion angle  $\chi$  of  $45^\circ$ , or, in other words, with no  $\delta$  overlap. With the bond length of 2.138(1) Å found for a twist angle of zero, the two extrema give a bond distance range of 0.054 Å on going from a full  $\delta$  bond to none at all.

The results of this analysis were refined in a subsequent study of eleven compounds, in which the relatively minor steric and electronic differences among the bridging ( $\text{P}^\wedge\text{P}$ ) and ( $\text{As}^\wedge\text{P}$ ) ligands were considered, and experiment-based corrections for the electronic factors were applied to the metal–metal distances.<sup>23</sup> When the resulting modified Mo–Mo distances were used in the analysis (Figure 7), the result was a straight-line fit with a correlation coefficient of 0.955 and intercepts corresponding to Mo–Mo = 2.128 Å for  $\chi = 0^\circ$  and 2.225 Å for  $\chi = 45^\circ$ . Thus, the change in the length of the metal–metal bond on passing from full  $\delta$  overlap to none at all was estimated

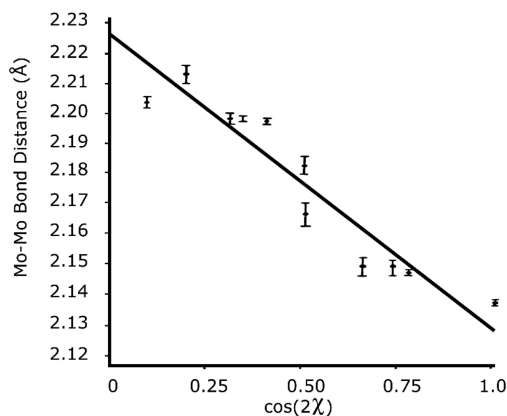


**Figure 7.** Variation of the Mo–Mo distances (Å) in  $\text{Mo}_2\text{X}_4(\text{PR}_3)_4$  and  $\text{Mo}_2\text{X}_4(\text{diphosphine})_2$  compounds, where  $X = \text{Cl}$  and  $\text{Br}$ , as a function of the internal rotation. An angle  $\chi$  of  $0^\circ$  represents an eclipsed configuration (b.o. = 4), while an angle  $\chi$  of  $45^\circ$  represents a staggered configuration (b.o. = 3). There are 11 data points. For additional details, see section 16.1.2 in ref 19.

to be 0.097 Å. An important lesson from these studies is that, even though the absolute values might not be as clear-cut, the experimental data unmistakably show that as rotation about the metal–metal bond increases toward the value of 45°, the  $\delta$  bond diminishes, as was initially suggested. We will come back later to how metal–metal bond distances change as the bond order diminishes by either the addition or removal of one electron, in our discussion of other techniques.

### SUPPORT OF THE $\delta$ BOND FROM PHOTOELECTRON SPECTRA

Photoelectron spectroscopy (PES) provides the most direct and least equivocal experimental information about valence electrons in molecules. Briefly, in a typical experiment, a photon ( $h\nu$ ) having a defined energy is used to remove an electron from a bound state. For practical reasons, the energy used is greater than that necessary to remove the electron from a neutral molecule in the gas phase. Thus, when the electron is ejected, it is in motion. The kinetic energy,  $E_K(e^-)$ , of the ejected electron is the quantity measured. Under these conditions, the ionization energy ( $E_I$ ) is given by the relationship  $E_I = h\nu - E_K(e^-)$ . In a representative spectrum, the bands show how electrons are removed from the outermost (less tightly held) to the innermost (more tightly held) shells upon irradiation of a gas with ultraviolet light. By convention, measurements of ionization energies must be made in the gas phase and are commonly given in units of electronvolts, where  $1 \text{ eV} = 1.6 \times 10^{-19} \text{ J}$ .<sup>24</sup>

Early work, done mainly in the Hillier and Lichtenberger laboratories, characterizing many quadruple-bonded species such as  $M_2X_8^{4-}$ ,  $M_2(\text{carboxylate})_4$ ,  $M_2(\text{formamidinate})_4$ ,  $M_2(\text{methylhydroxypyridinate})_4$ , where  $M = \text{Cr, Mo, and W}$ , has been reviewed.<sup>19,25</sup> A noteworthy study was carried out on the quadruple-bonded  $\text{Re}_2\text{Cl}_8^{2-}$  ion.<sup>26</sup> The spectrum shown in Figure 8 provides a direct picture of the occupied MOs. In the

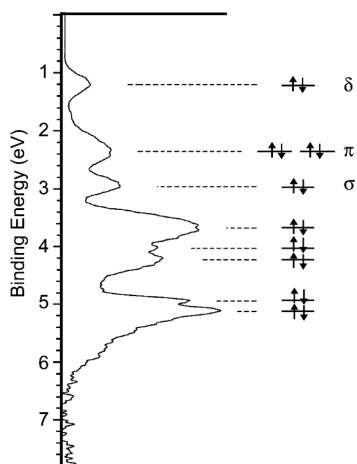


**Figure 8.** PES spectrum of the  $[\text{Re}_2\text{Cl}_8]^{2-}$  anion. Note that the lowest binding energy corresponds to electrons in the  $\delta$  bond followed by those in  $\pi$  and finally  $\sigma$ -type orbitals.

spectrum, the metal–metal- and metal–ligand-bonding MOs were clearly observed and distinguished.<sup>27</sup> It was found that the metal–metal-bonding MOs from the d orbitals ( $\delta$ ,  $\pi$ , and  $\sigma$ ) have low electron binding energies and yielded three well-resolved detachment bands that are followed by a plethora of peaks from other ionizations. This spectrum provides a distinct

connection between the proposed theoretical description in the initial paper<sup>13</sup> and experiment. It is important to point out that sometimes the analysis may be more complex, especially when the ligands are ionized at energies similar to those of the dimetal units. An example is that of the  $M_2(\text{DTolF})_4$  compounds, where DTolF is the anion of  $N,N'$ -di-*p*-tolylformamidine [ $\text{tolNC}(\text{H})\text{Ntol}$ ] and  $M$  is a group 6 element (Cr, Mo, and W) in which several formamidinate-based ionizations derived from the nitrogen  $p_\pi$  orbitals occur among the metal–metal  $\sigma$ ,  $\pi$ , and  $\delta$  ionization bands. Nevertheless, assignment of the main bands from the dimetal units is possible.<sup>28</sup> As an example, the spectrum of the dimolybdenum analogue in Figure 9 shows the lowest

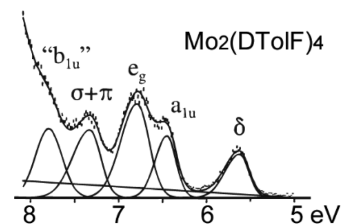
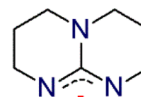


**Figure 9.** PES spectrum of  $\text{Mo}_2(\text{DTolF})_4$ . Note that the peak corresponding to the  $\delta$  bond is clearly visible, but the band for the  $\pi$  electrons is complicated by ionizations from the ligand. Deconvolution is necessary to identify the band.

ionization energy where that corresponding to the detachment of the electron in a  $\delta$  orbital is clearly isolated, but the band corresponding to the detachment of electrons in  $\pi$  MOs is more complex because of ionizations of the formamidinate ligands having similar energies. Nevertheless, mathematical deconvolution of the signal allows identification of the band corresponding to the dimetal unit. Another important PES study was done on compounds of the type  $M_2(\text{hpp})_4$  where  $M = \text{Cr, Mo, and W}$  (see Scheme 2). Of these compounds, the

### Scheme 2. Bicyclic Guanidinate Ligand Referred to in the Text as hpp<sup>a</sup>



<sup>a</sup>It represents the anion of 1,3,4,6,7,8-hexahydro-2*H*-pyrimido[1,2-*a*]pyrimidine. The N–C(N)–N core is what characterizes the guanidinate ligands. The two hydrogen atoms in each of the six methylene groups have been removed for clarity.

ditungsten species has the lowest ionization energy of any stable species (*vide infra*). It is even lower than that of elemental cesium, as detailed in the following section.

### DESTABILIZATION OF THE $\delta$ BOND LEADING TO STRONG REDUCING AGENTS

Some of the most commonly studied dimetal-bonded species are those containing dimolybdenum units. After scores of compounds with  $\text{Mo}_2^{n+}$  cores had been studied, there was a consensus that the predominant value of  $n$  was 4, i.e.,  $\text{Mo}_2^{4+}$ ; that is, these compounds possess eight metal-based electrons and thus a quadruple bond. Early on, there were multiple attempts to oxidize and isolate the singly oxidized tetracarboxylate or octahalide compounds because there was electrochemical evidence that  $\text{Mo}_2^{5+}$  species were attainable. After

some hard work, a handful were indeed isolated, with an example being 2,4,6-trisopropylphenyl carboxylate, TiPB, which was oxidized from  $\text{Mo}_2(\text{TiPB})_4$  to  $[\text{Mo}_2(\text{TiPB})_4]^+$ , i.e.,  $\text{Mo}_2^{4+} \rightarrow \text{Mo}_2^{5+}$ .<sup>29</sup> The species containing the  $\text{Mo}_2^{5+}$  core exhibited one unpaired electron. It was fully characterized by X-ray diffraction, electrochemistry, and EPR. The cation has a Mo–Mo distance of about 0.06 Å longer than that of the neutral molecule. It is important to note that, because the electron would be expected to be removed from a bonding  $\delta$  orbital, an increase in the metal-to-metal distance is expected, and thus this is consistent with the basic diagram and with the cation having a  $\sigma^2\pi^4\delta$  electronic configuration and a b.o. of 3.5. Also decisive is the information from EPR. Because there is one unpaired electron, an important question is whether this electron is in a ligand-based orbital or whether it occupies a metal-based MO. In the former case, a sharp signal with a  $g$  value similar to that of the free electron or of an organic radical ( $g = \sim 2.00$ ) would be expected. Instead, the EPR spectrum shows two  $g$  values,  $g_{\parallel} = g_{\perp} = 1.936$ , with hyperfine splitting due to the spin-active isotopes  $^{95}\text{Mo}$  and  $^{97}\text{Mo}$ . This evidence strongly suggests that the unpaired electron is in a metal-based MO. It should be noted that there are two  $g$  values because of the tetragonal core structure. In addition to the EPR data, the electronic spectrum shows a red shift of the lowest-energy band ( $\delta \rightarrow \delta^*$  transition) due to the loss in exchange energy upon going from the two-electron to the one-electron system.

After great difficulties were experienced in oxidizing  $\text{Mo}_2(\text{O}_2\text{CR})_4$  and isolating oxidized  $\text{Mo}_2(\text{O}_2\text{CR})_4^+$  species, a tremendous surprise emerged and new lessons were learned from the study of guanidinate compounds. These are species characterized by having an NC(N)N skeleton, where the central carbon atom is  $\text{sp}^2$ -hybridized. When the compound with a bicyclic guanidinate having two six-membered rings (referred to as hpp; Scheme 2) was prepared, its structure was that of an unremarkable paddlewheel compound. Curiously, the compound was difficult to handle because it appeared to decompose in aerobic conditions or in some common solvents. When a  $^1\text{H}$  NMR spectrum in  $\text{CD}_2\text{Cl}_2$  was attempted, there was nothing but broad signals characteristic of paramagnetic species. Crystallization from solution showed that the only species in solution was  $\text{Mo}_2(\text{hpp})_4\text{Cl}$ ,<sup>30</sup> whose structure is shown in Figure 10. Further exposure of the dichloromethane solution containing  $\text{Mo}_2(\text{hpp})_4\text{Cl}$  to air produced  $\text{Mo}_2(\text{hpp})_4\text{Cl}_2$ . The ease of formation of  $\text{Mo}_2^{5+}$  and  $\text{Mo}_2^{6+}$

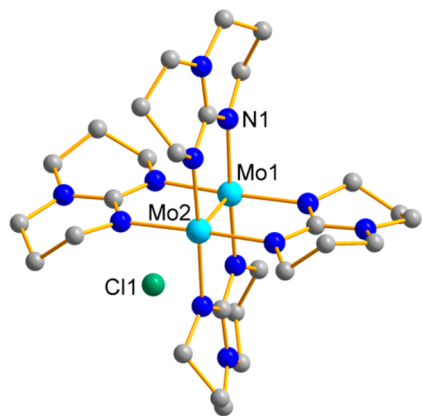


**Figure 10.** Structure of  $\text{Mo}_2(\text{hpp})_4\text{Cl}$ , with a M–M bond order of 3.5, showing the paddlewheel structure and a chlorine atom located at ca. 3.5 Å from Mo2 along the metal-to-metal axis.

species is in sharp contrast to what happens with carboxylate ( $\text{RCO}_2$ ) and even formamidinate  $[\text{RNC}(\text{H})\text{R}]$  analogues.

The Mo–Mo distance of 2.067(1) Å in  $\text{Mo}_2(\text{hpp})_4$  increases by about 0.05 Å in  $\text{Mo}_2(\text{hpp})_4\text{Cl}$  and by a similar amount upon further oxidation to  $\text{Mo}_2(\text{hpp})_4\text{Cl}_2$ , in accordance with what one would expect from the removal of an electron from a  $\delta$  orbital in each step. Both  $\text{Mo}_2(\text{hpp})_4$  and  $\text{Mo}_2(\text{hpp})_4\text{Cl}_2$  are diamagnetic; the former contains a quadruple bond, while the latter has a triple bond between the metal atoms. By contrast  $\text{Mo}_2(\text{hpp})_4\text{Cl}$  is paramagnetic, having a single unpaired electron and a b.o. of 3.5. Electrochemical studies highlighted the remarkable difference in the oxidation processes, as seen in Figure 11. For the carboxylate derivatives, the only observed

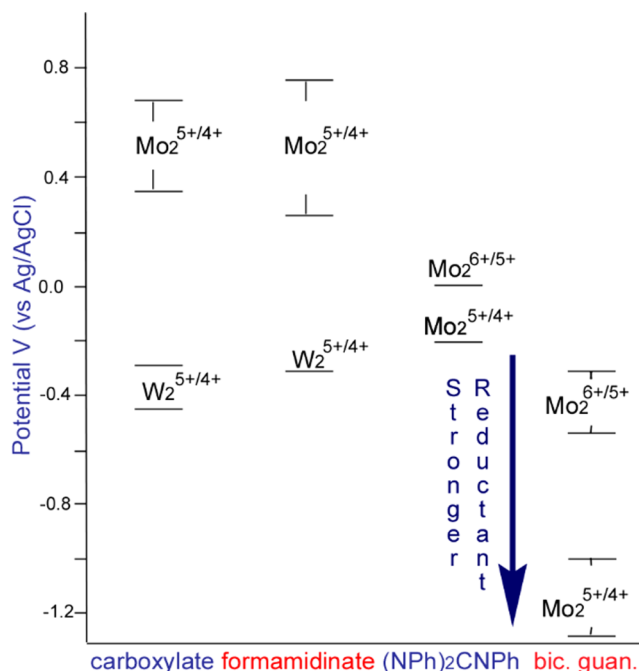


**Figure 11.** Electrochemical data for some quadruple-bonded paddlewheel compounds showing the large difference between carboxylate, formamidinate, and bicyclic guanidinate species. Not shown in the diagram are the potentials for  $\text{W}_2(\text{bicyclic guanidinate})_4$  compounds, which are in the ranges of  $-0.97$  to  $-0.99$  V for the  $\text{W}_2^{6+/5+}$  system and  $-1.81$  to  $-1.90$  V for the  $\text{W}_2^{5+/4+}$  system.

oxidation process is in the range of about 0.3–0.6 V vs Ag/AgCl (the specific value depends on the nature of the R group). However, for the hpp derivative, there were two processes observed at  $-0.44$  and  $-1.27$  V vs Ag/AgCl. Thus, for the  $\text{Mo}^{5+/4+}$  couple, there is a very large difference of ca. 1.5 V between the values for carboxylate compounds and those for compounds with bicyclic guanidates. The natural question is, why?

Before we pursue an answer, let us look at the tungsten analogues. Again, it was found that  $\text{W}_2(\text{hpp})_4$ <sup>31</sup> was extraordinarily easy to oxidize in chlorinated solvents. Analogous to the molybdenum compounds,  $\text{W}_2(\text{hpp})_4\text{Cl}$  and  $\text{W}_2(\text{hpp})_4\text{Cl}_2$  can also be isolated. Again, the W–W distance increases by about 0.05 Å with each oxidation step, in accordance with the removal of an electron from a  $\delta$  orbital. The electrochemical studies again show two oxidation waves, but these are at the very negative values of  $-0.97$  and  $-1.81$  V vs Ag/AgCl. Furthermore, PES studies show that the most external electron (i.e., that in a  $\delta$  orbital) is lost at the record

low ionization energy of 3.76(2) eV (vertical) and 3.51 (5) eV (onset). Remarkably, the ionization energy of  $W_2(\text{hpp})_4$  is even lower than that of elemental gaseous cesium (3.89 eV). It should be noted that  $W_2(\text{hpp})_4$  can reduce a large variety of compounds, e.g., TCNQ, fullerenes, and halogenated hydrocarbons, among others. However, there was a caveat in that the oxidized ditungsten species were generally insoluble and often difficult to remove from the reaction mixtures. This problem was resolved recently by attaching alkyl substituents to the hpp ligands, creating tetramethyl and tetraethyl derivatives (TMhpp and TEhpp).<sup>32</sup> The corresponding  $W_2(\text{TMhpp})_4$  and  $W_2(\text{TEhpp})_4$  compounds are very soluble, even in alkanes, and have even stronger reducing characteristics as well as slightly lower ionization energies. They are better reducing agents than the commonly used decamethylcobaltocene. Figure 12 shows the PES spectrum, structure, and differential pulse voltammogram for  $W_2(\text{TMhpp})_4$ .<sup>33</sup>

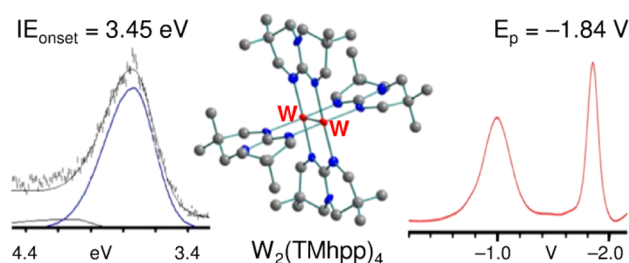


**Figure 12.** Photoelectron spectrum, structure, and differential pulse voltammogram of  $W_2(\text{TMhpp})_4$  showing the exceedingly low ionization energy (even less than that of cesium).

Answers to why these  $M_2(\text{hpp})_4$  derivatives lose electrons so easily were provided by density functional theory (DFT) calculations. It was found that the  $sp^2$ -hybridized core of the guanidinate ligand strongly interacts with the electrons in the  $\delta$  orbital, which destabilizes them. This symmetry-allowed interaction is thus responsible for the drop in the gas-phase ionization energy.<sup>31,34</sup> Importantly, without a  $\delta$  bond, such a decrease in the oxidation potential would not be possible. DFT studies of the tetraalkyl-substituted hpp derivatives also showed the existence of a strong relationship between the electrode potentials, gas-phase ionization energies, and solvation processes.<sup>32</sup>

### ■ FRACTIONAL BOND ORDERS: ARE THE UNPAIRED ELECTRONS IN METAL-BASED ORBITALS?

On the basis of the idealized MO diagram for  $D_{4h}$  species in Figure 5 and the formal bond order definition, one can see that whenever there is an odd number of electrons, there is a possibility that the dimetal units can be paramagnetic and that b.o. may be fractional. Indeed, the first complex with a fractional oxidation state,  $Re_2Cl_5(\text{CH}_3\text{SCH}_2\text{CH}_2\text{SCH}_3)_2$ , obtained from the reaction of the  $[Re_2Cl_8]^{2-}$  ion with  $\text{CH}_3\text{SCH}_2\text{CH}_2\text{SCH}_3$ , was discovered over 47 years ago.<sup>35</sup> The complex is best thought of as having a  $Re_2^{5+}$  core with a  $\sigma^2\pi^4\delta^2\delta^*$  electronic configuration. Additionally, we have already noted the example of  $[Mo_2(\text{TiBP})_4]^+$ , which has a  $Mo_2^{5+}$  core, seven metal-based electrons, a  $\sigma^2\pi^4\delta$  electronic configuration, and thus b.o. of 3.5.<sup>29</sup> Similarly, there is a series of rhenium compounds whose b.o. can vary from 3 to 3.5 to 4. An example is that of the series  $Re_2Cl_4(\text{dppm})_2$ ,  $Re_2Cl_5(\text{dppm})_2$ , and  $Re_2Cl_6(\text{dppm})_2$ , where  $\text{dppm} = 1,1$ -bis(diphenylphosphino)-

methane.<sup>36</sup> It should be noted that, in the paramagnetic compound  $Re_2Cl_5(\text{dppm})_2$ , the  $Re_2^{5+}$  core has a  $\sigma^2\pi^4\delta^2\delta^*$  electronic configuration. Interestingly, for some guanidinate  $Re_2^{n+}$  species, there are also two more accessible core configurations, with  $n = 7$  (b.o. = 3.5;  $7e$ )<sup>37</sup> and  $8$  (b.o. = 3;  $6e$ ).<sup>38</sup> Even though the formal bond order for  $n = 7$ , which is 3.5, is the same as that in  $Re_2^{5+}$ , the electronic configuration differs because the  $Re_2^{5+}$  species is *electron-rich*, with the outer electron in a  $\delta^*$  orbital, while the former is *electron-poor* with the outer electron in a  $\delta$  orbital. In this respect, it resembles  $Mo_2(\text{TiPB})_4^+$  (vide supra).<sup>29</sup> Other species with fractional bond orders are those having  $M_2^{5+}$  (15e), where  $M = \text{Pt}$  and  $\text{Pd}$ , with b.o. of 0.5,<sup>39</sup>  $M_2^{5+}$  (13e), where  $M = \text{Ir}$  and  $\text{Rh}$ , with b.o. of 1.5,<sup>40</sup> and  $Ru_2^{5+}$  (11e) with b.o. of 2.5.<sup>41</sup> Some additional species with b.o. of 3.5 are  $Cr_2^{5+}$ ,<sup>42</sup>  $Re_2^{7+}$ ,<sup>37</sup>  $Os_2^{7+}$ ,<sup>43</sup> and  $Tc_2^{5+}$ .<sup>44</sup> Again, there is a difference in the electronic configuration between  $Re_2^{7+}$  and  $Os_2^{7+}$  because the former has seven metal-based electrons, while the latter has nine ( $\sigma^2\pi^4\delta$  vs  $\sigma^2\pi^4\delta^2\delta^*$ ).

In this section, we have been using the term *metal-based electrons* liberally and without experimental support. It is important to keep in mind that having an unpaired electron in a metal-containing species does not necessarily mean that the electron is in a metal-based orbital because it is always possible that a given species may instead contain organic radicals, i.e., species with unpaired ligand-based electrons. Indeed, this is why there is a very extensive literature dealing with the so-called noninnocent ligands, and thus it is often very difficult to assign oxidation states when dealing with metal-containing species.<sup>45</sup>

Because of this, Al sought an experimental technique that could unambiguously clarify this issue. EPR is this ideal technique. In this way, a long-time collaboration with Naresh Dalal and the National High Magnetic Field Laboratory emerged. Many of the results are given in the references above, but here we will use one compound to illustrate how this approach was useful in finding a definitive answer. The reader will note that again a team of collaborators is often essential in science. The example we will use is that of the  $[Re_2(\text{hpp})_4Cl_2]^+$  species, which has a  $Re_2^{7+}$  core ( $7e$ ).<sup>37</sup>

Upon preparation of the quadruple-bonded  $Re_2(\text{hpp})_4Cl_2$  compound, electrochemical measurements showed two waves at 0.58 and 0.733 V (vs  $\text{Ag}/\text{AgCl}$ , with the  $\text{Fc}/\text{Fc}^+$  couple appearing at 0.440 V under similar conditions). Up to that point, there were no examples of oxidations that would produce  $Re_2^{7+}$  species. Instead, there were a large number of examples of reductions.<sup>19</sup> A natural question arose as to whether these were indeed oxidation processes. The thinking at the time included a fear that such an unprecedented state, obtained by the removal of electrons, would be accompanied by an increase of the positive charge of the metal atoms, and this, in turn, had the potential to shrink the size of the d orbitals. Such a reduction in size would then diminish the overlap between the orbitals. With lesser orbital overlap, there was a risk that the relatively weak  $\delta$  bond would be lost and thus the oxidation might be occurring on a ligand. Therefore, resolving the issue of where the electrons were situated was essential. Are the electrons on the metal or on the ligand?

The first thing that was done was to carry out a reaction using a ferrocenium salt ( $\text{Cp}_2\text{FePF}_6$ ) as a reactant. Because the  $\text{Fc}/\text{Fc}^+$  couple appeared at 0.440 V and the first electrochemical event for  $Re_2(\text{hpp})_4Cl_2$  was at 0.58 V, isolation under such conditions would demonstrate the existence of a  $Re_2^{7+}$  species

and would also show that a  $\text{Re}_2^{8+}$  species was indeed possible. In this way,  $[\text{Re}_2(\text{hpp})_4\text{Cl}_2]\text{PF}_6$  was obtained, and its structure showed a Re–Re distance that was longer than that of the  $\text{Re}_2^{6+}$  precursor by 0.035 Å. This paramagnetic (by one electron) compound showed an electronic spectrum with bands at around 550 nm, consistent with a transition from a  $\delta$  bond with b.o. of  $1/2$ . These were encouraging results, especially the lengthening of the Re–Re distance, but they were not definitive because one could argue that the lengthening of the metal-to-metal bond could be due to an increase in the electrostatic repulsion and a decrease in the orbital overlap due to an increase in the positive charge.

The strongest support for a metal-based oxidation came from EPR studies of  $[\text{Re}_2(\text{hpp})_4\text{Cl}_2]\text{PF}_6$ . At ambient temperature and using the standard X-band field strength ( $\sim 9.5$  GHz), the spectrum of the solid consists of a single, exchange-narrowed, featureless line at  $g = 1.7421$  with a peak-to-peak line width of 600 G. This was important because, as mentioned earlier, an organic-type radical would be expected to show a sharp line with  $g \approx 2.00$ . Similar observations were made for  $[\text{Re}_2(\text{hpp})_4(\text{SO}_3\text{CF}_3)_2](\text{SO}_3\text{CF}_3)$  at 290 K and a field of 9.3 GHz, where the  $g$  value was similar (1.782). A typical spectrum is shown in Figure 13. However, a more desirable measurement

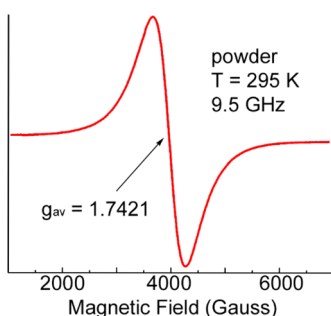


**Figure 13.** X-band EPR spectrum of a powder of  $[\text{Re}_2(\text{hpp})_4\text{Cl}_2]\text{PF}_6$ . Note the broadness of the band as opposed to what would be expected from an organic free radical (very sharp signal with a  $g$  value of ca. 2.00).

is that done in solution in a frozen matrix. When compounds are placed in solution, solid-state effects such as dipolar and magnetic effects are diminished because the solute molecules are now farther apart. Under these conditions, there is a dramatic change. The isotropic spectrum from  $\text{CH}_2\text{Cl}_2$  glasses (340 K), shown in Figure 14, consists of 11 hyperfine peaks from coupling to two equivalent rhenium nuclei ( $I = 5/2$ ). The structure arises from the effect of two natural spin-active isotopes:  $^{185}\text{Re}$ , 37.4% abundance,  $g_n = 1.2748$ ,  $I = 5/2$ , and  $^{187}\text{Re}$ , 62.6% abundance  $g_n = 1.2878$ ,  $I = 5/2$ , both having approximately the same hyperfine coupling constants under the experimental conditions used. A better spectral definition is obtained by decreasing the temperature to 153 K and increasing the field to 34 GHz, upon which all 33 expected lines are observed, as shown in Figure 15. The observation of hyperfine structure directly attributed to the rhenium atom provides unambiguous evidence that the unpaired electron resides in a metal-based MO. Such evidence is now available for many other systems with fractional bond orders.

Another interesting study is that in which the quadruple-bonded  $\text{Tc}_2\text{Cl}_8^{2-}$  dianion was reduced to produce the anion  $\text{Tc}_2\text{Cl}_8^{3-}$ .<sup>44</sup> The frozen-solution EPR spectra from X- and Q-band frequencies show the presence of an unpaired electron

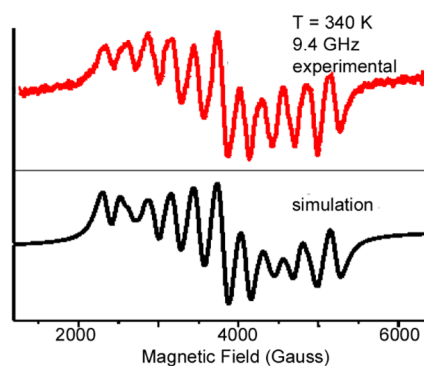


**Figure 14.** Experimental and simulated EPR spectra ( $\nu = 9.4$  GHz) of a solution of  $[\text{Re}_2(\text{hpp})_4\text{Cl}_2]\text{PF}_6$ . The isotropic 11-line hyperfine structure is due to rhenium isotopes. The spectrum was collected using a  $\text{CH}_2\text{Cl}_2$  solution.

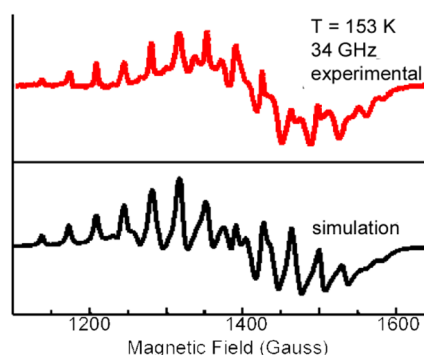


**Figure 15.** Experimental and simulated EPR spectra ( $\nu = 34$  GHz) for  $[\text{Re}_2(\text{hpp})_4\text{Cl}_2]\text{PF}_6$  which contains a  $\text{Re}_2^{7+}$  core. The 33-line anisotropic hyperfine structure is due to rhenium isotopes. The spectrum was gathered in a frozen  $\text{CH}_2\text{Cl}_2$  glass.

with a hyperfine structure due to two equivalent  $^{99}\text{Tc}$  nuclei ( $I = 9/2$ ) and with  $g_{\parallel} = 1.912$ ,  $g_{\perp} = 2.096$ ,  $A_{\parallel} = 1.66 \times 10^{-4} \text{ cm}^{-1}$ , and  $A_{\perp} = 62.7 \times 10^{-4} \text{ cm}^{-1}$ . This is consistent with the unpaired electron being in a metal-based MO for this species, which has an electron-rich b.o. of 3.5, an electronic configuration of  $Q\delta^*$ , and a  $\text{Tc}_2^{5+}$  core.<sup>46</sup> Interestingly, these species provide one of the exceptions to how the metal–metal distances change as b.o. diminishes. For the quadruple-bonded species  $\text{Tc}_2\text{Cl}_8^{2-}$ , which has a  $\text{Tc}_2^{6+}$  core, the Tc–Tc distance is 2.147(4) Å,<sup>47</sup> while that for the  $\text{Tc}_2\text{Cl}_8^{3-}$  anion, with its  $\text{Tc}_2^{5+}$  core and b.o. of 3.5, decreases to 2.117(2) Å in  $\text{K}_3\text{Tc}_2\text{Cl}_8 \cdot n\text{H}_2\text{O}$ <sup>48</sup> and 2.13(1) Å in  $(\text{NH}_4)_3\text{Tc}_2\text{Cl}_8 \cdot 2\text{H}_2\text{O}$ .<sup>49</sup> This is contrary to what is normally observed, namely, that the metal–metal bond distance increases as the bond order decreases. The shortening has been rationalized by considering that, for these species, as the bond order increases, the positive charge of the technetium atoms increases, and thus there is an increase in the repulsion between the metal atoms. Unfortunately, there have been no additional studies to complement the data from this pair of compounds, and other influences (e.g., hydrogen bonding in the presence of a highly negatively charged anion and water and/or ammonium species) cannot be ruled out. Thus, as a general principle, one cannot consider the bond order as the only variable when analyzing variations in metal–metal bond distances.



## ■ AROMATICITY AND ELECTRONIC COMMUNICATION INVOLVING $\delta$ BONDS

Efforts to link two or more species containing dimetal units through a linker, similar to that of a Creutz–Taube ion ( $\{[\text{Ru}(\text{NH}_3)_5](\text{pyz})[\text{Ru}(\text{NH}_3)_5]\}^{5+}$ ) in Figure 16,<sup>50</sup> have

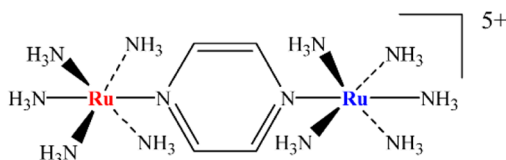
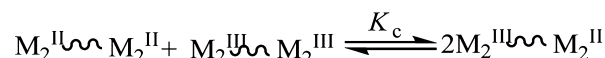


Figure 16. Creutz–Taube ion.

produced a very large number of architectures ranging from pairs, loops, triangles, and squares to more complex units, some examples of which are shown in Scheme 3. Because the background information has been provided in various accounts,<sup>51</sup> we will not provide much additional detail but will instead limit our discussion to a few specific examples that clearly show how electrons in  $\delta$  bonds can be involved in electronic communication. The basic premise was that by studying the electrochemistry, accompanied by structures, EPR, and electronic spectra, information could be obtained on how two units communicate with the aid of a linker and how the linker affects such communication. It is easily seen that if a linker favors communication, when an electron is removed from the first dimetal unit, it will follow that a second electron removal (oxidation) would be more difficult because the second dimetal unit would “feel” the positive charge more effectively than when the linker acts as an insulator. In the opposite case, when a linker acts as an insulator, removal of a second electron would not be significantly affected and the potential for its removal would be similar to that of the first process. Practically, in the first situation (a linker that favors communication), one expects to see two clearly separated oxidation waves displaying a significant difference between the first and second oxidation processes. In the other case, in which the linker acts as an insulator, the difference would be small and quite often not measurable within experimental error.

On the basis of the difference in the electrochemical events ( $\Delta E_{1/2}$ ), one can calculate the so-called comproportionation constant, i.e.,  $K_C$ :<sup>52</sup>

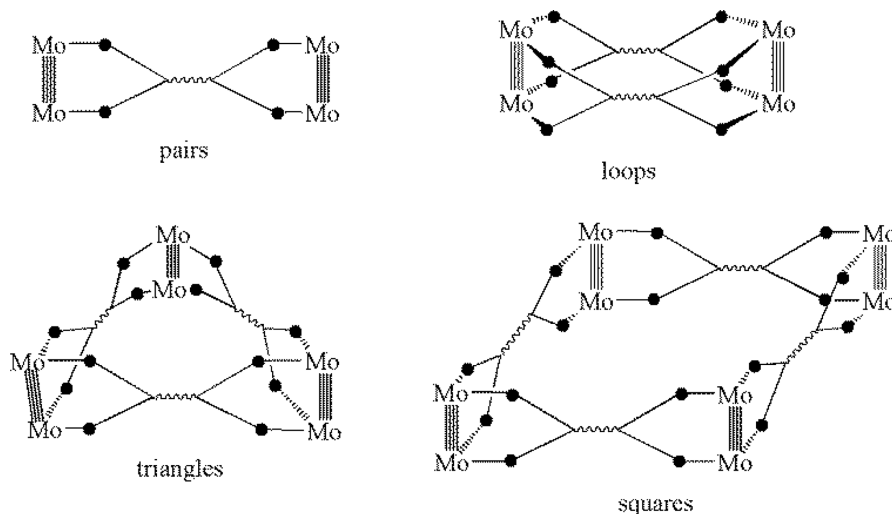


$$K_C = e^{\Delta E_{1/2}/25.69}$$

An elegant example is provided by a system having two isomers containing two quadruple-bonded  $\text{Mo}_2(\text{DAniF})_3$  [ $\text{DAniF} = N,N'$ -di-*p*-anisylformamidate,  $(\text{Ani})\text{NC}(\text{H})\text{N}(\text{Ani})$ ] units linked by a diaryloxamidate ( $\text{Ar} = p\text{-MeOC}_6\text{H}_4$ ) linker.<sup>53</sup> Depending on synthetic conditions, two different isomers ( $\alpha$  and  $\beta$ ) can be isolated in high purity. Importantly, because of steric effects, they do not interconvert. Two electrons can be removed from each isomer in a stepwise manner to give the corresponding singly and doubly oxidized species.<sup>54</sup> The singly oxidized species,  $\alpha^+$  and  $\beta^+$ , are shown in Figure 17. It should be noted that for the  $\alpha$  form ( $D_{2d}$ ) the two dimolybdenum units are essentially perpendicular to each other, while in the  $\beta$  form ( $D_{2h}$ ), those units are essentially parallel to each other.

The X-ray crystallographic analyses show unambiguously that the mixed-valence species in the  $\alpha^+$  form has an unsymmetrical structure, with the Mo–Mo bond distances corresponding to localized  $\text{Mo}_2^{4+}$  and  $\text{Mo}_2^{5+}$  units, whereas in the  $\beta^+$  form, there are two essentially identical  $[\text{Mo}_2]$  units, as shown in Table 1. Consistently, these compounds also exhibit different features in the near-IR (NIR) spectra: While the  $\alpha^+$  form has a featureless spectrum in this region, the  $\beta^+$  form presents an intense absorption at low energy, which is centered at ca.  $4730\text{ cm}^{-1}$ . This band, shown in Figure 18, is conventionally referred to as a metal-to-metal intervalence charge-transfer band but is better described as a HOMO–1  $\rightarrow$  SOMO transition in a fully delocalized molecule. An additional oxidation process produces the two doubly oxidized compounds  $\alpha^{2+}$  and  $\beta^{2+}$ . Magnetic studies showed a strikingly different behavior. The  $\alpha^{2+}$  species is paramagnetic because of the weakness of interactions of the two localized  $\text{Mo}_2^{5+}$  units, but the  $\beta^{2+}$  form is diamagnetic

Scheme 3. Some Architectures Obtained Using Dimolybdenum Units and Various Linkers<sup>a</sup>



<sup>a</sup>The ancillary formamidate ligands spanning the  $\text{Mo}_2$  units have been removed for clarity.

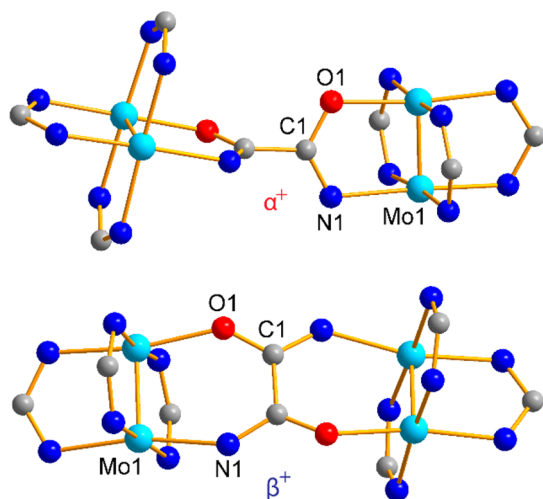


**Figure 17.** Structures of the  $\alpha^+$  and  $\beta^+$  isomers in  $[\text{Mo}_2]$ -(diphenyloxamidate) $[\text{Mo}_2]$ . For visual simplicity, the aryl groups in both the ancillary formamidinate ligands and the oxamidate linker have been removed from each of the nitrogen atoms (dark blue).

because of the pairing of the electrons in the two  $\text{Mo}_2^{5+}$  units. The small value of  $\Delta E_{1/2}$  (ca. 190 mV) for the neutral  $\alpha$  form is equivalent to a  $K_C$  of  $10^3$ , while that for the  $\beta$  form is 6 orders of magnitude higher ( $K_C$  of about  $10^9$ ).

The EPR spectra of both the  $\alpha^+$  and  $\beta^+$  forms have similar  $g$  values of about 1.95 (see the inset in Figure 18). Furthermore, the presence of a hyperfine structure due to the  $^{95,97}\text{Mo}$  ( $I = 5/2$ ) isotopes supports the hypothesis that the unpaired electron is in a metal-based MO, and thus for both forms, the unpaired electrons are assigned to those in  $\delta$  orbitals. An important difference, however, is that the coupling constants for the two singly oxidized species are quite different, with that of  $\alpha^+$  ( $A = 21 \times 10^{-4} \text{ cm}^{-1}$ ) being about twice that of  $\beta^+$  ( $A = 11 \times 10^{-4} \text{ cm}^{-1}$ ). It should be noted that the  $A$  value for the parent  $[\text{Mo}_2(\text{DAniF})_4]^+$  is similar to that of  $\alpha^+$ , and this again indicates that  $\alpha^+$  has little electronic communication through the linker, while the smaller value of  $A$  for  $\beta^+$  supports the existence of strong electronic communication, as does the large difference of about  $10^6$  in the  $K_C$  values.

It is worthwhile noting the resemblance that the two fused six-membered rings in the  $\beta^+$  and  $\beta^{2+}$  complexes have with naphthalene, where an aromatic system is clearly present. Therefore, the  $\beta^{2+}$  species behaves as a heteronaphthalene system.

Another example that goes a bit further in showing how electrons in  $\delta$ -type orbitals can interact strongly through appropriate linkers (in a manner that can lead to aromaticity) is provided by  $[\text{Mo}_2]_2(\mu\text{-EH})_2$  species ( $\text{E} = \text{O}, \text{S}$ ) and  $[\text{Mo}_2] = \text{Mo}_2(\text{formamidinate})_3$ .<sup>55</sup> These species can be oxidized with the concomitant removal of hydrogen atoms. The key feature is the observation that for each  $[\text{Mo}_2]$  group there are two methine hydrogen atoms [the hydrogen atom on the central carbon atom of the  $\text{NC}(\text{H})\text{N}$  moiety] that are trans to each other and only one that is cis to both of the first type. In other words, two

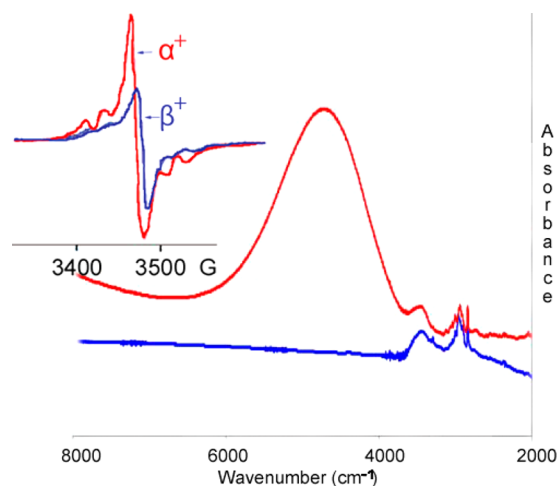


**Figure 18.** NIR spectrum of the  $\alpha^+$  (red trace) and  $\beta^+$  (blue) isomers of  $[\text{Mo}_2]$ (diphenyloxamidate) $[\text{Mo}_2]$ . The upper left inset shows the X-band EPR spectra.

methine hydrogen atoms are in the plane of the dimetal units, and four methine H atoms are perpendicular to that plane. In these systems, the  $[\text{Mo}_2]_2(\mu\text{-EH})_2$  and  $[\text{Mo}_2]_2(\mu\text{-E})_2$  species are diamagnetic and thus amenable to  $^1\text{H}$  NMR studies. The spectra are shown in Figure 19.

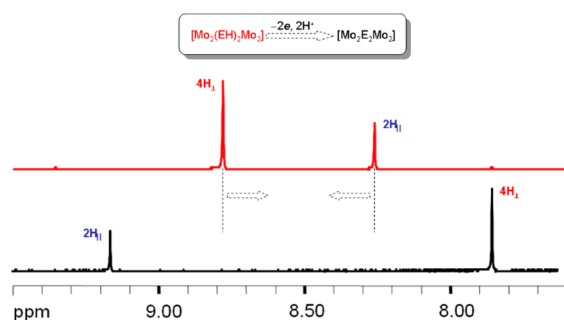


**Figure 19.** NMR spectra of the methine region of  $[\text{Mo}_2](\text{SH})_2[\text{Mo}_2]$  (top) and the corresponding oxidized species  $[\text{Mo}_2](\text{S})_2[\text{Mo}_2]$  (bottom). Note the switch in relative position, upon oxidation, of the proton signals from the groups perpendicular and parallel to the plane that include the six-membered ring  $\text{Mo}_2\text{S}_2\text{Mo}_2$ .

What is evident is that the signals for  $\text{H}_{\parallel}$  in the protonated (unoxidized) species are at a lower field than those for  $\text{H}_{\perp}$ , while the opposite is true for the oxidized species. The latter has  $2n + 4$  electrons in the six-membered ring that contains the four molybdenum atoms plus the two sulfur atoms. This can be explained by considering the magnetic anisotropy induced by aromaticity of the  $[\text{Mo}_2]_2(\mu\text{-E})_2$  species, much in the same way that we explain the fact that the hydrogen signals in the NMR spectrum of benzene are at a much lower field than those in an alkane such as hexane. This is illustrated in Figure 20.

**Table 1.** Mo–Mo Bond Distances (Å) in the  $\alpha$  and  $\beta$  Forms

compound	$\alpha$	$\beta$	$\alpha^+$	$\beta^+$	$\alpha^{2+}$	$\beta^{2+}$
Mo1–Mo2	2.0927(8)	2.0947(4)	2.0920(6)	2.1116(7)	2.1236(8)	2.1449(8)
Mo3–Mo4	same	same	2.1291(6)	2.1140(6)	2.1254(8)	2.1416(8)

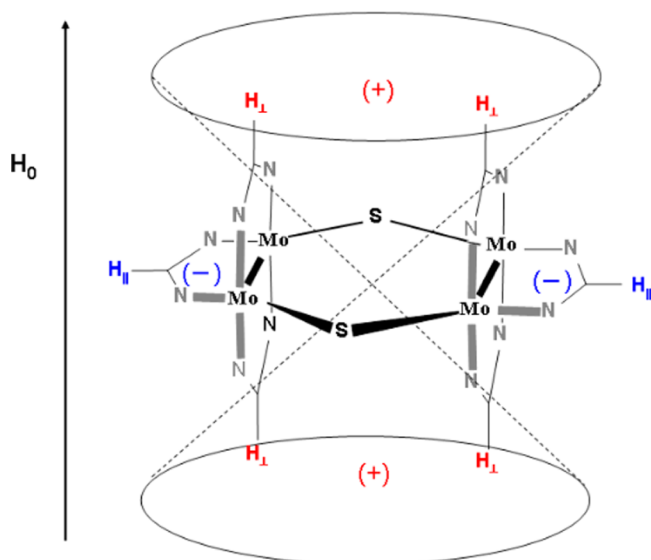


**Figure 20.** Representation of the signals from the hydrogen atoms in the positive region shift to higher fields, while those in the negative region shift to lower fields (higher ppm values).

### EXCEPTIONS TO THE SIMPLE ORBITAL ORDERING DIAGRAM: THE DIRUTHENIUM CASE

Up to this point, we have emphasized the benefits and utility of the MO diagram in Figure 5; however, this is not always straightforward. The diagram works only to a first approximation, but, nevertheless, it is quite satisfying how well it works most of the time.

One of the situations for which the diagram has had difficulties explaining experimental data is that of diruthenium units. A specific case is that of compounds containing  $\text{Ru}_2^{5+}$  species. A simple electron count gives 11 metal-based electrons and thus b.o. of 2.5. Should the scheme be valid, one would write the electronic configuration as  $\sigma^2\pi^4\delta^2\delta^{*2}\pi^*$  and predict that such compounds would exhibit magnetism consistent with the presence of one unpaired electron. However, experimental evidence sometimes reveals that there is indeed one unpaired electron, but in many other cases, there are three.<sup>19</sup> The natural question is why? The differences likely result from a small difference in energy, or near-degeneracy, between the  $\delta^*$  and  $\pi^*$  orbitals that sometimes can even go as far as an inversion in energy.<sup>19,56</sup> Thus, for moieties with three unpaired electrons, the electronic configuration would be expected to be  $\sigma^2\pi^4\delta^2\pi^*\delta^*$ , in which case each of the antibonding orbitals would have one unpaired electron (a total of three). Unfortunately, the situation could be even more complicated because of zero-field splitting, which can be measured by the so-called  $D$  values obtained from EPR spectroscopy or magnetometry (SQUID measurements). This effect deals with the difference in energy between spin states caused by a Zeeman effect, e.g., in biradicals.<sup>57</sup> Because of such complications, historically the electronic configuration of  $\text{Ru}_2^{5+}$  species was referred to as being  $\text{Q}(\delta^*\pi^*)^3$ , where, as before,  $\text{Q}$  is the underlying  $\sigma^2\pi^4\delta^2$  configuration. With this nomenclature, it was understood that the three electrons in the frontier orbitals are distributed in some fashion between the  $\delta^*$  and  $\pi^*$  orbitals.

Examining the situation in more detail, one may note that because of the similarity in energy of the HOMO and SOMO the provenance of the ground state for these species with an 11-

electron core might be any of three configurations:  $\text{Q}\delta^{*2}\pi^*$ ,  $\text{Q}\pi^{*2}\delta^*$ , and  $\text{Q}\pi^{*3}$ . Moreover, two states, each arising from a different one of these configurations, might be so close in energy that a Boltzmann-type temperature dependence of their partial populations could come into play. For these configurations, magnetic measurements may distinguish between the  $\text{Q}\pi^{*2}\delta^*$  state, which has three unpaired electrons, but not the other two ( $\text{Q}\delta^{*2}\pi^*$  and  $\text{Q}\pi^{*3}$ ), which have one unpaired electron each.

This is where new experimental evidence was needed, and this was provided by temperature-dependent crystallography. The temperature dependence, or lack thereof, of the Ru–Ru bond length can show whether or not close-lying states that derive from different configurations are involved, and if so, what pairs of configurations are pertinent. The reasoning behind this is that a change in the metal-to-metal bond distance would be anticipated if an electron moves from a  $\delta^*$  to a  $\pi^*$  orbital because a  $\pi^*$  orbital would be expected to have more antibonding character than a  $\delta^*$  orbital and thus one would expect to see an increase in the bond distance. In addition, this could differentiate cases where magnetic measurements show a change in the magnetic moment because of zero-field splitting because in such cases there would be no change in the electronic configuration. Thus, one then would not expect to see significant changes in the metal-to-metal distances.

So what do the experiments show? Let us begin by examining the case of a species with a  $\text{Ru}_2^{6+}$  core,  $(\text{Ru}_2(\text{hpp})_4\text{Cl}_2)$ ; 10-electron system), in which the electronic configuration could be  $\text{Q}\delta^{*2}$  or  $\text{Q}\pi^{*2}$ . Magnetic measurements showed that the compound possesses two unpaired electrons at room temperature, but the magnetic susceptibility drops to essentially zero at 2 K.<sup>58</sup> Does this mean that the electronic configuration is changing from one with two unpaired electrons ( $\text{Q}\pi^{*2}$ ) to  $\text{Q}\delta^{*2}$ ? If that were to be the case, we should see a decrease in the metal-to-metal distances as the temperature decreases (electrons would be moving from a  $\pi^*$  to a  $\delta^*$  orbital). However, crystal structures done at 27, 50, 100, 213, and 296 K show an insignificant variation in such distances of only 0.0009 Å, with that at 27 K being 2.3233(9) Å. Because of the long Ru–Ru distance, it was concluded that the two external electrons were in  $\pi^*$  orbitals. For comparison, the unsupported Ru–Ru distance in the  $\text{Ru}_2^{5+}$  species  $\text{Na}_3[\text{Ru}(\text{Cl}_4\text{Cat})_4(\text{THF})]$  [where  $\text{Cl}_4\text{Cat}$  = tetrachlorocatecholate, which has two nonbridging catecholate ligands and an axial tetrahydrofuran (THF) molecule] is only 2.273(1) Å,<sup>59</sup> and this distance decreases even further to 2.2233(6) Å upon a one-electron oxidation that leads to the removal of the electron in the  $\pi^*$  orbital. Scheme 4 shows a diagram of the states arising from a  $\text{Q}\pi^{*2}$  configuration and the splitting of the ground state  $^3\text{A}_{2g}$ .

Going back to the 11-electron  $\text{Ru}_2^{5+}$  species, let us look at what happens when two isomers of the type  $\text{Ru}_2(\text{formamidinate})_4\text{Cl}$  are examined by variable-temperature crystallography.<sup>60</sup> The formamidinates are  $\text{DAni}^p\text{F}$  in its para and meta forms ( $\text{DAni}^p\text{F}$  and  $\text{DAni}^m\text{F}$ , respectively).

The magnetic results are summarized in Figure 21 and those from the variable-temperature crystallographic studies in Figure 22. In the para isomer, the Ru–Ru distance increases by 0.05 Å as the temperature changes from ambient to 27 K, while that of the meta isomer remains essentially constant. The drop in the magnetism of the meta isomer is typical of a zero-field splitting, while that of the para isomer, in which  $\chi T$  reaches a value of only 1.6 at 300 K and with decreasing temperature declines to a value of 0.5 at 2 K, is consistent with a spin crossover and thus a

Scheme 4. MO Diagram of the States Arising from a  $\sigma^2\pi^4\delta^2\pi^{*2}$  ( $Q\pi^{*2}$ ) Electronic Configuration and the Splitting of the Ground State  $^3A_{2g}$

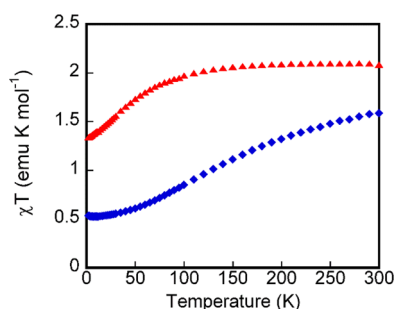
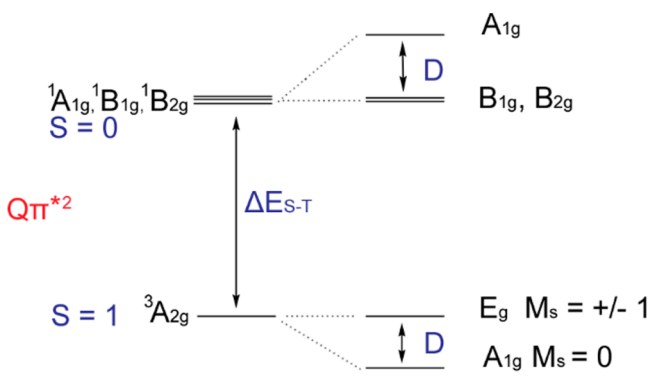


Figure 21. Magnetism of the para (in blue diamonds) and meta (in red triangles) isomers of  $\text{Ru}_2(\text{DAniF})_4\text{Cl}$  as a function of the temperature.

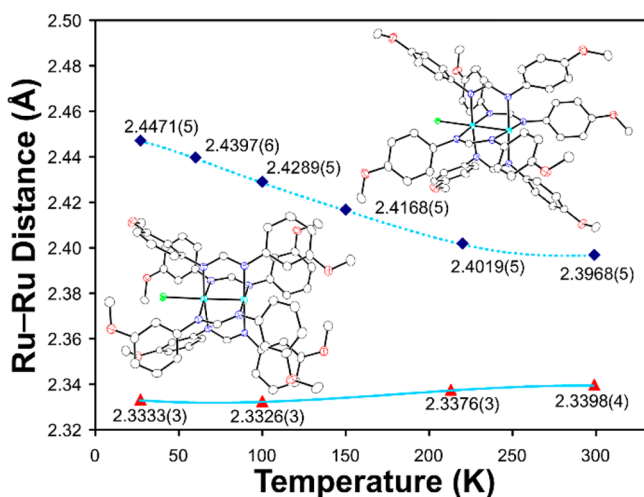


Figure 22. Variation of the Ru–Ru distances in  $\text{Ru}_2(\text{DAniF})_4\text{Cl}$  isomers as a function of the temperature. The data for the para isomer are in blue diamonds, while those for the meta isomer are in red triangles.

change in the electronic configuration from  $Q\pi^{*2}\delta^*$  at ambient temperature to  $Q\pi^{*3}$  at 2 K.

Finally, we note that there are a large number of  $\text{Ru}_2^{6+}$  species with very long metal-to-metal-distances ( $>2.5$  Å), most of which have four formamidate bridging ligands and acetylide axial ligands whose electronic configurations have been postulated to be  $\pi^4\delta^2\pi^{*4}$ .<sup>19</sup> The basis for this proposed configuration is that, owing to the long Ru–Ru separation, the  $\sigma$  bond is lost; the loss of the  $\sigma$  bond, in turn, has been

attributed to a strong interaction with the  $\pi$ -donating acetylide ligands.

The lesson behind these examples is that, even though the scheme in Figure 5 is often valid and is a helpful predictor, it should not be used blindly. Experimental techniques and results as well as theoretical calculations must always serve as a guide.

## CHIRALITY IN SPECIES WITH METAL-TO-METAL BONDS

A review of this topic has been published,<sup>61</sup> so we will focus on the key concepts and studies that illustrate how chiroptical properties can provide insight into the electronic structures of compounds with metal–metal bonds.

Chirality enters into the field of metal–metal bonds from two viewpoints that are quite distinct, both conceptually and practically. From the point of view of metal–metal bonding per se, introducing chirality in an opportune fashion opens a window to exploring the finer aspects of the electronic structure of the molecule. In a conceptually opposite direction, the special properties of metal–metal-bonded compounds, especially their catalytic properties, can be enhanced by chirality, which in the case of catalysts introduces the possibility of stereodirection in catalytic reactions.

The latter topic has been reviewed in depth.<sup>62</sup> Here we will focus on the former aspect of chiral metal–metal-bonded compounds, namely, the manner in which chirality can permit insight into the electronic structure of the bond.<sup>63</sup>

Moscovitz described “case I” and “case II” chromophores, in which case I was an intrinsically chiral chromophore and case II was an achiral chromophore with chiral surroundings.<sup>64</sup> In the context of circular dichroism (CD) spectroscopy, which is the most natural technique for exploring the electronic structures of chiral molecules, each of these cases gives rise to CD transitions in its own way, with each being quite different from the other. When a metal–metal bond is the chromophore, the information that can be obtained from CD spectra is different in the two cases.

The differences and the nature of the transitions can be most easily understood with reference to the rotational strength (the analogue of the transition moment) for CD spectroscopy. Similar to the transition moment  $I$  for electronic spectroscopy, which is a dipole moment (with a translation operator  $\mu$  or  $P$ , eq 1) for a transition from  $\psi_i$  to  $\psi_j$ , or from  $a$  to  $b$ , the analogue of the transition moment for CD, the rotational strength  $R$ , is the imaginary part,  $\text{Im}$ , of the product of an electric dipole moment (translation operator  $P$ ) and a magnetic dipole moment (rotation operator  $M$ , eq 2, in which  $\theta$  is the angle between the electric and magnetic moments).

$$I \propto \int \psi_i \mu \psi_j d\tau \quad \text{or} \quad \langle a | P | b \rangle \quad (1)$$

$$R = \text{Im} \langle a | P | b \rangle \langle b | M | a \rangle = \mu m \cos \Theta \quad (2)$$

When the chromophore is chiral, its point group symmetry consists of only pure rotations, and each of the three translations  $x$ ,  $y$ , and  $z$  transforms as the same irreducible representation, as does the corresponding rotation  $R_x$ ,  $R_y$ , and  $R_z$ , respectively.<sup>65</sup> That is,  $x$  and  $R_x$  transform the same way, and so forth. This has the consequence that, for every electronic transition that is symmetry-allowed—i.e., the integral in eq 1 is nonzero—the corresponding CD transition is also allowed (eq 2).

The compound  $\text{Mo}_2\text{Cl}_2(\text{S,S-dppb})_2$  [ $\text{S,S-dppb} = 2\text{S,3S-bis(diphenylphosphino)butane}$ ; Figure 23], which was studied

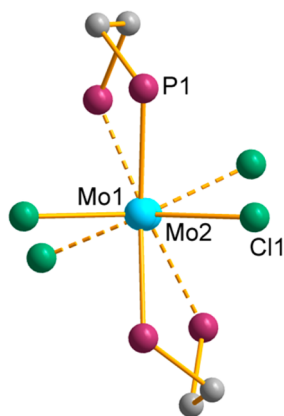


**Figure 23.** Core of the molecule  $\text{Mo}_2\text{Cl}_2(\text{S,S-dppb})_2$  showing the twist about the Mo–Mo bond [average P–Mo–Mo–P torsion angle of  $24(2)^\circ$ ]. The chromophore, which is viewed with the metal–metal bond going into the paper, has  $D_2$  symmetry.

along with its bromo analogue, provides a good example of a case I chromophore.<sup>66</sup> The chromophore has  $D_2$  symmetry, so the  $\delta$ – $\delta^*$  transition is allowed in the electronic spectrum with  $z$  polarization and is ( $z$ ,  $R_z$ )-allowed in the CD spectrum. Both spectra show the peak at  $13700\text{ cm}^{-1}$ . Its sign in the CD spectrum is negative. Using a simple charge-distribution model, Al and collaborators associated the sign of the CD band with the sense of twist around the metal–metal bond. This result demonstrated that if a reasonable assumption could be made regarding the magnitude of the twist—specifically, whether it was greater than or less than  $45^\circ$ —then the sign of the  $\delta$ – $\delta^*$  transition in the CD spectrum served to reveal the sense of the twist. This established a useful CD-based diagnostic for the direction of torsion in this class of compounds.

When the chromophore is intrinsically achiral, with a point group that includes improper symmetry elements (case II), the corresponding translation and rotation operators (e.g.,  $\alpha$  and  $R_x$ ) do not transform as the same irreducible representation of the point group of the chromophore, and in the absence of chiral perturbation from the surroundings, the CD rotational strength given in eq 2 must be zero. When a transition is electronically allowed, with the first integral in eq 2 nonzero, then the magnetic dipole moment integral (second part of eq 2) must be zero, and vice versa, a transition that is “magnetically allowed” (second integral nonzero) must be electronically prohibited, giving no transition in the CD.

As described by Mason, the chiral surroundings perturb the excited states in the corresponding transitions in such a way that some of the “electronic excited state” is mixed into the “magnetic excited state” and vice versa, thus breaking the selection rules and enabling both electronic and magnetic transitions.<sup>67</sup> For electronic transitions, this produces a CD peak corresponding to an allowed transition in the electronic spectrum, with the added value that the CD transition also has a sign. However, in addition, this perturbation process reveals magnetic transitions, which are not seen in the electronic spectrum. These are new peaks and can, in principle, add invaluable information for interpretation of the electronic structure of the compound.

Al and some of us examined the electronic and CD spectra of two paddlewheel compounds with Rh–Rh single bonds and chiral bridging carboxylate ligands, namely,  $\text{Rh}_2[(\text{S})\text{-mandelate}]_4(\text{EtOH})_2$  and  $\text{Rh}_2[(\text{R})\text{-}\alpha\text{-methoxy-}\alpha\text{-phenylacetate}]_4(\text{THF})_2$ .<sup>68</sup> We will consider the mandelate compound, although the analysis is similar for the two. The chromophore, with nominal  $D_{4h}$  symmetry (Figure 24), is perturbed by the

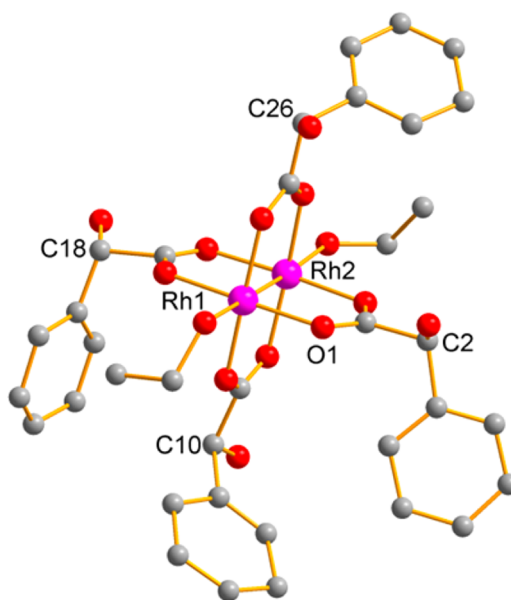


**Figure 24.** One molecule of  $\text{Rh}_2[(\text{S})\text{-mandelate}]_4(\text{EtOH})_2$ . The chromophore has  $D_{4h}$  symmetry and is surrounded by chiral ligands. The four labeled carbon atoms are chiral. The hydrogen atoms are not shown.

chiral ligands, giving rise to negative CD peaks corresponding to the transition energies observed in the electronic spectrum (electronically allowed,  $17100$  and  $22500\text{ cm}^{-1}$ ), and with additional CD peaks with no corresponding purely electronic transitions (Figure 25). The latter are the “magnetically allowed” transitions whose presence is interpreted alongside the electronic transitions. Special importance was accorded the broad, positive CD band at  $20000\text{ cm}^{-1}$ , which was interpreted as being based on two magnetically allowed transitions whose

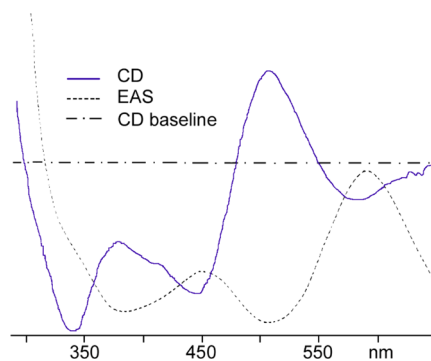


**Figure 25.** CD and EAS spectra for  $\text{Rh}_2[(\text{S})\text{-mandelate}]_4(\text{EtOH})_2$ . The electronic transitions at  $585$  and  $445\text{ nm}$  ( $17100$  and  $22500\text{ cm}^{-1}$ ) have analogues with negative signs in the CD spectrum. The positive CD peak at  $\sim 500\text{ nm}$  ( $20000\text{ cm}^{-1}$ ) has no counterpart in the electronic spectrum; it is a magnetically allowed transition. The CD baseline corresponds to  $\Delta\epsilon = 0$ .

corresponding excited states were the origins of the perturbations that, in turn, endowed the electronically allowed transitions with their intensity.<sup>68</sup> The details of the analysis, which made use of a MO calculation of the electronic structure of the molecule, are beyond our present scope; however, the important point is that interpretation of the CD spectrum, involving four transitions and leading to correct descriptions of their origins, energies, and CD signs, gave more insight into the electronic structure of the chromophore than was available from an interpretation based solely on the two electronic transition energies available from the electronic absorption (EAS) spectrum.

## ■ PARENTHESES

Writing a *historical* account on the work done by Al and his group on the quadruple bond has been a joy, but we need to acknowledge that one of the frustrating aspects is having to leave out many outstanding contributions by other laboratories such as those of Harry Gray and his students and Malcolm Chisholm and collaborators. For those in the field, who does not remember the work on optical spectroscopy entitled “The delta star: What the energies and intensities mean?”<sup>69</sup> This topic also led to Dan Nocera’s ideas on how to effect two-electron redox processes upon excitation to the singlet  $\delta \rightarrow \delta^*$ .<sup>70</sup> More recently, Chisholm has been studying mixed valence in ground-state metal cations and organic anions and photoexcited states of molecular systems,<sup>71</sup> and he has also shown that the lifetimes of metal-to-ligand charge-transfer states arising from photoinduced metal  $\delta$  to ligand  $\pi^*$  orbitals have long lifetimes that have allowed for time-resolved studies of both the singlet and triplet states.<sup>72</sup> In many ways, it is disappointing not to be able to dedicate a long section to the work on quintuple bonds, but this is an area that a new generation will be able to expand upon.<sup>73</sup> Finally, it is worth keeping in mind that hundreds of references are provided in ref 19.

## ■ CONCLUDING REMARKS

What is now a half-century of research into the quadruple bond and its  $\delta$  component began with an unexpected discovery inspired by the application of bonding concepts to the results of a single-crystal structure determination. Al Cotton had not set out to discover the quadruple bond. However, his solid scientific base, and especially his strong command of, and easy adaptability to, new physical and theoretical techniques, permitted him to conceive and direct the research that would reveal many intricacies of the nature of the  $\delta$  bond. The most important experimental techniques included photoelectron and EPR spectroscopies and single-crystal X-ray structure analysis. Al Cotton was a master of the inductive use of structural results, deriving some of the most important conclusions about metal–metal bonding from a series of structures in which geometric variations could be associated with the properties of the bonds. The study of the variation of the metal–metal bond length with increasing twist about the bond, and the quantitative association of this variation with the progressive loss of the  $\delta$  component, is an excellent example of how synthesis, structure, and theory can be coordinated to provide each with added value in the form of a rigorous conclusion regarding bonding. This and other aspects of the development of our knowledge of the  $\delta$  bond still serve as examples of how a productive, multifaceted research program based on both discovery and

design can resolve complex scientific problems. Through this account, Al’s passion for teaching lives on.

## ■ AUTHOR INFORMATION

### Corresponding Authors

\*E-mail: falvello@unizar.es.

\*E-mail: foxman1@brandeis.edu.

\*E-mail: murillo@tamu.edu.

### Notes

The authors declare no competing financial interest.

### Biographies



Larry R. Falvello received a B.S., summa cum laude, in Chemistry from Duke University in 1976 and did graduate studies at Cambridge University (Certificate of Post-Graduate Study with Olga Kennard and Ph.D., 1979, with Malcolm Gerloch). After a 2-year postdoctoral stay at Cambridge University (Malcolm Gerloch), he was a postdoc (1981–1982) and Staff Scientist (1982–1991) at the Laboratory for Molecular Structure and Bonding at Texas A&M University. From 1991, he has been Professor of Inorganic Chemistry at the University of Zaragoza. His research group studies the preparation and physical and structural properties of transition-metal complexes in molecular crystals. Falvello is a member of the International Union of Crystallography Journals Commission and is Deputy Section Editor of *Acta Crystallogr., Sect. C* and Associate Editor of *Comments Inorg. Chem.*



Bruce M. Foxman received his B.S. in Chemistry, with distinction, from Iowa State University in 1964, where he carried out research under the direction of John G. Verkade. His Ph.D. work at Massachusetts Institute of Technology with F. Albert Cotton, completed in 1968, included work on triple- and quadruple-bonded rhenium complexes. He was a Research Fellow in Alan Sargeson’s group at the Australian National University from 1968 to 1972, where he studied reaction kinetics of cobalt(III) complexes and developed

novel ideas on solid-state reactivity. He moved to Brandeis University in 1972, where he has studied the reactions of inorganic and organometallic complexes in the solid state for over 40 years. He has held invited visiting appointments at Oxford University, Max-Planck-Institut für Polymerforschung, University of Birmingham, and Université Louis Pasteur.



Carlos A. Murillo studied chemistry at the University of Costa Rica and Texas A&M University, where he received his Ph.D. in 1973 with F. Albert Cotton. He then did postdoctoral work with Malcolm H. Chisholm at Princeton University. He went then back to Costa Rica, where he quickly moved to the rank of Professor. In 1991, he moved to Texas A&M University as director of the Laboratory for Molecular Structure and Bonding, and in 2007, he took a position as program director in the Division of Chemistry at the U.S. National Science Foundation. He has continued his research on compounds with multiple bonds between metal atoms as an adjunct professor at Texas A&M University and the University of Texas at El Paso, where he is an adjunct professor. He is a Fellow of the American Association for the Advancement of Science and a charter member of the Costa Rican Academy of Sciences.

## ACKNOWLEDGMENTS

C.A.M. thanks Texas A&M University and the National Science Foundation (IR/D support). L.R.F. thanks the Ministerio de Ciencia e Innovación (Spain) for support under Grant MAT2011-27233-C02-01 with cofinancing from the European Union Regional Development Fund (FEDER), and B.M.F. acknowledges the National Science Foundation for support.

## REFERENCES

- (1) (a) Peligot, E. C. *R. Acad. Sci.* **1844**, *19*, 609. (b) Peligot, E. *Ann. Chim. Phys.* **1844**, *12*, 528.
- (2) Cotton, F. A.; George, J. W.; Waugh, J. S. *J. Chem. Phys.* **1958**, *28*, 994.
- (3) Kraihanzel, C. S.; Cotton, F. A. *Inorg. Chem.* **1963**, *2*, 533.
- (4) (a) Cotton, F. A. *Inorg. Chem.* **1966**, *5*, 1083. (b) Cotton, F. A. *Inorg. Chem.* **2002**, *41*, 643.
- (5) (a) Fackler, J. P., Jr.; Cotton, F. A. *J. Chem. Soc.* **1960**, 1435. (b) Calderazzo, F.; Cotton, F. A. *Inorg. Chem.* **1962**, *1*, 30.
- (6) For example, see: Cotton, F. A.; Wilkinson, G.; Murillo, C. A.; Bochmann, M. *Advanced Inorganic Chemistry*, 6th ed.; John Wiley & Sons, Inc.: New York, 1999.
- (7) Bertrand, J. A.; Cotton, F. A.; Dollase, W. A. *Inorg. Chem.* **1963**, *2*, 1166.
- (8) Cotton, F. A.; Mague, J. T. *Inorg. Chem.* **1964**, *3*, 1402.
- (9) Cotton, F. A.; Mague, J. T. *Inorg. Chem.* **1964**, *3*, 1094.
- (10) (a) Cotton, F. A.; Lippard, S. J. *J. Am. Chem. Soc.* **1964**, *86*, 4497. (b) Cotton, F. A.; Lippard, S. J. *Inorg. Chem.* **1964**, *3*, 59.

- (11) Bennett, M. J.; Cotton, F. A.; Foxman, B. M. *Inorg. Chem.* **1968**, *7*, 1563.
- (12) Al's autobiography provides an excellent resource for additional background. See: Cotton, F. A. *My Life in the Golden Age of Chemistry: More Fun than Fun*; Elsevier Inc.: Waltham, MA, in press.
- (13) Cotton, F. A.; Curtis, N. F.; Harris, C. B.; Johnson, B. F. G.; Lippard, S. J.; Mague, J. T.; Robinson, W. R.; Wood, J. S. *Science* **1964**, *145*, 1305.
- (14) Cotton, F. A.; Curtis, N. F.; Robinson, W. R. *Inorg. Chem.* **1965**, *4*, 1696.
- (15) Cotton, F. A.; Foxman, B. M. *Inorg. Chem.* **1968**, *7*, 2135.
- (16) Eakins, J. D.; Humphreys, D. G.; Mellish, C. E. *J. Chem. Soc.* **1963**, 6013.
- (17) Cotton, F. A.; Bratton, W. K. *J. Am. Chem. Soc.* **1965**, *87*, 921.
- (18) Lawton, D.; Mason, R. J. *J. Am. Chem. Soc.* **1965**, *87*, 921.
- (19) For example, see: *Multiple Bonds between Metal Atoms*, 3rd ed.; Cotton, F. A., Murillo, C. A., Walton, R. A., Eds.; Springer Science and Business Media, Inc.: New York, 2005.
- (20) Theoretically, metal–metal bonds can be highly multiconfigurational, unlike bonds between carbon, nitrogen, and oxygen atoms.
- (21) Campbell, F. L., III; Cotton, F. A.; Powell, G. L. *Inorg. Chem.* **1984**, *23*, 4222.
- (22) Cotton, F. A.; Fanwick, P. E.; Fitch, J. W.; Glicksman, H. D.; Walton, R. A. *J. Am. Chem. Soc.* **1979**, *101*, 1752.
- (23) Campbell, F. L., III; Cotton, F. A.; Powell, G. L. *Inorg. Chem.* **1985**, *24*, 4384.
- (24) For the general background on PES, see: Lichtenberger, D. L.; Kellogg, G. E. *Acc. Chem. Res.* **1987**, *20*, 379.
- (25) (a) Cotton, F. A.; Norman, J. G., Jr.; Stults, B. R.; Webb, T. R. *J. Coord. Chem.* **1976**, *5*, 217. (b) Garner, C. D.; Hillier, I. H.; Knight, M. J.; MacDowell, A. A.; Walton, I. B.; Guest, M. F. *J. Chem. Soc., Faraday Trans.* **1980**, *76*, 885. (c) Lichtenberger, D. L.; Johnston, R. L. In *Metal–Metal Bonds and Clusters in Chemistry and Catalysis*; Fackler, J. P., Jr., Ed.; Plenum Press: New York, 1990; pp 275–298.
- (26) Wang, X. B.; Wang, L. S. *J. Am. Chem. Soc.* **2000**, *122*, 2096.
- (27) It is worth noting that in this experiment the  $[\text{Re}_2\text{Cl}_8]^{2-}$  species is produced from a salt solution using an electrospray ion source and then a mass spectrometer to capture and then separate the dianion from all other ions. After ions accumulated in the gas phase, a laser source is employed to detach the electron. Because of this, the electron comes out with a relatively high kinetic energy relative to the photon energy. In this example, the measured energy corresponds to the electron affinity of the neutral species, as opposed to the ionization energy when neutral species are used.
- (28) Lichtenberger, D. L.; Lynn, M. A.; Chisholm, M. H. *J. Am. Chem. Soc.* **1999**, *121*, 12167.
- (29) Cotton, F. A.; Hillard, E. A.; Murillo, C. A. *Inorg. Chem.* **2002**, *41*, 1639.
- (30) Cotton, F. A.; Daniels, L. M.; Murillo, C. A.; Timmons, D. J.; Wilkinson, C. C. *J. Am. Chem. Soc.* **2002**, *124*, 9249.
- (31) Cotton, F. A.; Gruhn, N. E.; Gu, J.; Huang, P.; Lichtenberger, D. L.; Murillo, C. A.; Van Dorn, L. O.; Wilkinson, C. C. *Science* **2002**, *298*, 1971.
- (32) Chiarella, G. M.; Cotton, F. A.; Durivage, J. C.; Lichtenberger, D. L.; Murillo, C. A. *J. Am. Chem. Soc.* **2013**, *135*, 17889.
- (33) For more details and references on the use of various bicyclic guanidates with quadruple-bonded compounds, see: Murillo, C. A. *Aust. J. Chem.* **2014**, *67*, in press.
- (34) (a) Cotton, F. A.; Donahue, J. P.; Gruhn, N. E.; Lichtenberger, D. L.; Murillo, C. A.; Timmons, D. J.; Van Dorn, L. O.; Villagrán, D.; Wang, X. *Inorg. Chem.* **2006**, *45*, 201. (b) Cotton, F. A.; Durivage, J. C.; Gruhn, N. E.; Lichtenberger, D. L.; Murillo, C. A.; Van Dorn, L. O.; Wilkinson, C. C. *J. Chem. Phys. B* **2006**, *110*, 19793.
- (35) Bennett, M. J.; Cotton, F. A.; Walton, R. A. *Proc. R. Soc. London* **1968**, *A303*, 175.
- (36) (a) Barder, T. J.; Cotton, F. A.; Lewis, D.; Schwotzer, W.; Tetric, S. M.; Walton, R. A. *J. Am. Chem. Soc.* **1984**, *106*, 2882. (b) Barder, T. J.; Cotton, F. A.; Dunbar, K. R.; Powell, G. L.; Schwotzer, W.; Walton, R. A. *Inorg. Chem.* **1985**, *24*, 2550.

- (37) (a) Cotton, F. A.; Dalal, N. S.; Huang, P.; Ibragimov, S. A.; Murillo, C. A.; Piccoli, P. M. B.; Ramsey, C. M.; Schultz, A. J.; Wang, X.; Zhao, Q. *Inorg. Chem.* **2007**, *46*, 1718. (b) Chiarella, G. M.; Cotton, F. A.; Dalal, N. S.; Murillo, C. A.; Wang, Z.; Young, M. D. *Inorg. Chem.* **2012**, *51*, 5257. (c) Berry, J. F.; Cotton, F. A.; Huang, P.; Murillo, C. A. *Dalton Trans.* **2003**, 1218.
- (38) Chiarella, G. M.; Cotton, F. A.; Murillo, C. A. *Chem. Commun.* **2011**, 47, 8940.
- (39) For example, see: Berry, J. F.; Bill, E.; Bothe, E.; Cotton, F. A.; Dalal, N. S.; Ibragimov, S. A.; Kaur, N.; Liu, C. Y.; Murillo, C. A.; Nellutla, S.; North, J. M.; Villagrán, D. J. *Am. Chem. Soc.* **2007**, *129*, 1393 and references cited therein.
- (40) For example, see: (a) Cotton, F. A.; Lin, C.; Murillo, C. A. *Inorg. Chem.* **2000**, *39*, 4574 and cited references therein. (b) Berry, J. F.; Cotton, F. A.; Huang, P.; Murillo, C. A.; Wang, X. *Dalton Trans.* **2005**, 3713.
- (41) For example, see: Cheng, W.-Z.; Cotton, F. A.; Dalal, N. S.; Murillo, C. A.; Ramsey, C. M.; Ren, T.; Wang, X. *J. Am. Chem. Soc.* **2005**, *127*, 12691.
- (42) Cotton, F. A.; Dalal, N. S.; Hillard, E. A.; Huang, P.; Murillo, C. A.; Ramsey, C. M. *Inorg. Chem.* **2003**, *42*, 1388.
- (43) Cotton, F. A.; Chiarella, G. M.; Dalal, N. S.; Murillo, C. A.; Wang, Z.; Young, M. D. *Inorg. Chem.* **2010**, *49*, 319.
- (44) Cotton, F. A.; Pedersen, E. *Inorg. Chem.* **1975**, *14*, 383.
- (45) For example, see: (a) Lu, C. C.; Bill, E.; Weyhermüller, T.; Bothe, E.; Wieghardt, K. *J. Am. Chem. Soc.* **2008**, *130*, 3181. (b) Ringerberg, M. R.; Kokatam, S. L.; Heiden, Z. M.; Rauchfuss, T. B. *J. Am. Chem. Soc.* **2008**, *130*, 788. (c) Das, D.; Sarkar, B.; Mondal, T. K.; Mobin, S. M.; Fiedler, J.; Kaim, W.; Lahiri, G. K. *Inorg. Chem.* **2011**, *50*, 7090.
- (46) Used for electronic configurations,  $Q$  signifies  $\sigma^2\pi^4\delta^2$ .
- (47) Cotton, F. A.; Daniels, L. M.; Davison, A.; Orvig, C. *Inorg. Chem.* **1981**, *20*, 3051.
- (48) (a) Koz'min, P. A.; Novitshaya, G. N. *Russ. J. Inorg. Chem.* **1972**, *17*, 1652. (b) Cotton, F. A.; Shive, L. W. *Inorg. Chem.* **1975**, *14*, 2032.
- (49) (a) Cotton, F. A.; Bratton, W. K. *J. Am. Chem. Soc.* **1965**, *87*, 921. (b) Bratton, W. K.; Cotton, F. A. *Inorg. Chem.* **1970**, *9*, 789.
- (50) For example, see: (a) Creutz, C.; Ford, P. C.; Mayer, T. J. *Inorg. Chem.* **2006**, *45*, 7059. (b) Stebler, A.; Ammeter, J. H.; Fűrholz, U.; Ludi, A. *Inorg. Chem.* **1984**, *23*, 2764. (c) Bunker, B. C.; Drago, R. S.; Hendrickson, D. N.; Richman, R. M.; Kessel, S. L. *J. Am. Chem. Soc.* **1978**, *100*, 3805.
- (51) (a) Cotton, F. A.; Lin, C.; Murillo, C. A. *Acc. Chem. Res.* **2001**, *34*, 759. (b) Cotton, F. A.; Lin, C.; Murillo, C. A. *Proc. Natl. Acad. Sci. U.S.A.* **2002**, *99*, 4810. (c) Chisholm, M. H.; Gustafson, T. L.; Turro, C. *Acc. Chem. Res.* **2013**, *46*, 529. (d) Chisholm, M. H.; Macintosh, A. M. *Chem. Rev.* **2005**, *105*, 2949.
- (52) The expression for  $K_C$  can be easily derived from the thermodynamic relationships  $\Delta G = -RT \ln K = -nFE$ .
- (53) Cotton, F. A.; Liu, C. Y.; Murillo, C. A.; Villagrán, D.; Wang, X. *J. Am. Chem. Soc.* **2003**, *125*, 13564.
- (54) Cotton, F. A.; Liu, C. Y.; Murillo, C. A.; Zhao, Q. *Inorg. Chem.* **2007**, *46*, 2604.
- (55) Fang, W. J.; He, Q.; Tan, Z. F.; Liu, C. Y.; Lu, X.; Murillo, C. A. *Chem.—Eur. J.* **2011**, *17*, 10288.
- (56) An analogy is the electronic structure of simple, gaseous dinuclear species such as  $B_2$ ,  $C_2$ ,  $N_2$ , and  $O_2$  for which the MO ordering may show variations in the  $\sigma^*$  and  $\pi^*$  ordering.
- (57) For additional details, see ref 41.
- (58) Cotton, F. A.; Murillo, C. A.; Reibenspies, J. H.; Villagrán, D.; Wang, X.; Wilkinson, C. C. *Inorg. Chem.* **2004**, *43*, 8373.
- (59) Kondo, M.; Hamatami, M.; Kitagawa, S. *J. Am. Chem. Soc.* **1998**, *120*, 455.
- (60) Angaridis, P.; Cotton, F. A.; Murillo, C. A.; Villagrán, D.; Wang, X. *J. Am. Chem. Soc.* **2005**, *127*, 5008.
- (61) Cotton, F. A.; Murillo, C. A. *Eur. J. Inorg. Chem.* **2006**, 4209.
- (62) See Chapter 13 by D. J. Timmons and M. P. Doyle in ref 19.
- (63) When unpolarized UV/vis light passes through a given substance, absorption can occur if the frequency is capable of triggering electronic transitions, e.g.,  $d-d$ ,  $\pi-\pi^*$ , and  $n-\pi^*$  transitions. If regular, unpolarized UV/vis light passes through enantiomers, the spectrum is the same for either the *R* or *S* enantiomer. On the other hand, if areas of the spectrum where the enantiomers absorb are irradiated with polarized UV/vis light, then the chiral centers affect left- and right-circularly polarized light (lcpl or rcpl) differently. The small but measurable absorptions can be observed in what are commonly referred to as CD spectra. Because such spectra measure differences, these can be positive or negative in magnitude. Importantly, for pairs of enantiomers, the spectra are mirror images, and thus a maximum for an *R* enantiomer will produce a minimum for an *S* enantiomer, but both will have the same absolute value. The entity that gives rise to the absorption of electromagnetic radiation is referred to as the chromophore.
- (64) Moscovitz, A. *Tetrahedron* **1961**, *13*, 48.
- (65) Cotton, F. A. *Chemical Applications of Group Theory*, 3rd ed.; John Wiley & Sons: New York, 1990.
- (66) (a) Agaskar, P. A.; Cotton, F. A.; Fraser, I. F.; Peacock, R. D. *J. Am. Chem. Soc.* **1984**, *106*, 1851. (b) Agaskar, P. A.; Cotton, F. A.; Fraser, I. F.; Manojlovic-Muir, L.; Muir, K. W.; Peacock, R. D. *Inorg. Chem.* **1986**, *25*, 2511.
- (67) Mason, S. F. *Q. Rev. Chem. Soc.* **1963**, *17*, 20.
- (68) Agaskar, P. A.; Cotton, F. A.; Falvello, L. R.; Han, S. *J. Am. Chem. Soc.* **1986**, *108*, 1214.
- (69) Hopkins, M. D.; Gray, H. B.; Miskowski, V. M. *Polyhedron* **1987**, *6*, 705. This article is one of many interesting reviews and original works published in a special issue dedicated to advances in the chemistry of metal–metal bonds up to that year.
- (70) Cotton, F. A.; Nocera, D. G. *Acc. Chem. Res.* **2000**, *33*, 483.
- (71) Chisholm, M. H.; Lear, B. J. *Chem. Soc. Rev.* **2011**, *40*, 5254.
- (72) Chisholm, M. H.; Gustafson, T. L.; Turro, C. *Acc. Chem. Res.* **2013**, *46*, 529.
- (73) For example, see: (a) Wolf, R.; Ni, C.; Nguyen, T.; Brynda, M.; Long, G. J.; Sutton, A. D.; Fischer, R. C.; Fettingner, J. C.; Hellman, M.; Pu, L.; Power, P. P. *Inorg. Chem.* **2007**, *46*, 11277. (b) Roos, B. O.; Borin, A. C.; Gagliardi, L. *Angew. Chem., Int. Ed.* **2007**, *46*, 1469. (c) Carrasco, M.; Curado, N.; Maya, C.; Peloso, R.; Rodríguez, A.; Ruiz, E.; Alvarez, S.; Carmona, E. *Angew. Chem., Int. Ed.* **2013**, *52*, 11. (d) Rudd, P. A.; Liu, S.; Planas, N.; Bill, E.; Gagliardi, L.; Lu, C. C. *Angew. Chem., Int. Ed.* **2013**, *52*, 16 and references cited therein.